NOTICE

The quality of this microform is heavily dependent upon the quality of the original thesis submitted for microfilming. Every effort has been made to ensure the highest quality of reproduction possible.

If pages are missing, contact the university which granted the degree.

Some pages may have indistinct print especially if the original pages were typed with a poor typewriter ribbon or if the university sent us an inferior photocopy.

Reproduction in full or in part of this microform is governed by the Canadian Copyright Act, R.S.C. 1970, c. C-30, and subsequent amendments.

AVIS

La qualité de cette microforme dépend grandement de la qualité de la thèse soumise au microfilmage. Nous avons tout fait pour assurer une qualité supérieure de reproduction.

S'il manque des pages, veuillez communiquer avec l'université qui a conféré le grade.

La qualité d'impression de certaines pages peut laisser à désirer, surtout si les pages originales ont été dactylographiées à l'aide d'un ruban usé ou si l'université nous a fait parvenir une photocopie de qualité inférieure.

La reproduction, même partielle, de cette microforme est soumise à la Loi canadienne sur le droit d'auteur, SRC 1970, c. C-30, et ses amendements subséquents.

UNIVERSITY OF ALBERTA

VERIFYING A LUMPED-PARAMETER MODEL FOR PREDICTING AIRBORNE DUST CONCENTRATIONS IN A VENTILATED ENCLOSURE

BY

GAO WA

A thesis submitted to the Faculty of Graduate Studies and Research in partial fulfillment of the requirements for the degree of MASTER OF SCIENCE.

DEPARTMENT OF AGRICULTURAL ENGINEERING

Edmonton, Alberta

SPRING 1992

ISBN 0-315-73145-1

UNIVERSITY OF ALBERTA

RELEASE FORM

NAME OF AUTHOR: GAO WA

TITLE OF THESIS: VERIFYING A LUMPED-PARAMETER MODEL FOR PREDICTING AIRBORNE DUST CONCENTRATIONS IN A VENTILATED ENCLOSURE

DEGREE: MASTER OF SCIENCE

YEAR THIS DEGREE GRANTED: SPRING 1992

#6 – 10726 – 84 Av
Edmonton, Alberta
Gao Wa

DATE: Dec. 18 1991

UNIVERSITY OF ALBERTA

FACULTY OF GRADUATE STUDIES AND RESEARCH

The undersigned certify that they have read, and recommend to the The Faculty of Graduate Studies and Research for acceptance, a thesis entitled VERIFYING A LUMPED-PARAMETER MODEL FOR PREDICTING AIRBORNE DUST CONCENTRATIONS IN A VENTILATED ENCLOSURE submitted by GAO WA in partial fulfillment of the requirements for the degree of MASTER OF SCIENCE.

.....John Feddes.....

J. J. R. Feddes

.....

J. J. Leonard

.....R. T. Hardin.....

R. T. Hardin

Date:.....12 DEC 91.....1991

ABSTRACT

The principle objective of this project was to verify a mathematical model which was derived for describing the dynamic behavior of airborne dust undergoing turbulent diffusive and gravitational deposition in any location of a ventilated airspace from the standpoint of a lumped-parameter approximation by using swine dust as a test dust.

Average equilibrium airborne dust concentrations were predicted as a function of ventilation and dust generation rates, Time-dependent airborne dust concentrations at a designated location (or lump), also were predicted from ventilation and dust generation rates. The model calculation was solved as a 3-D lumped form of control volumes representing conservation of airflow rate. The results showed that: (1) when compared with previous results with talcum powder used as a test dust, the discrepancy between the predictions made by the model and those measured was greater, (2) the greatest deviations from the predicted values occurred at the medium ventilation rates. The particle size analysis showed that the swine dust used in this study has an average aerodynamic diameter of 2 μm, and 95% of the dust particles are less than 5 μm in size while approximately 45% of the dust particles are approximately 2 μm in diameter.

The statistical analysis of the data revealed that

three ventilation rates (300, 900, and 1500 m^3/hr) used throughout the experiment significantly affected the airborne dust concentrations. Three dust generation rates, when expressed as $533x10^6$, $554x10^6$, and $665x10^6$ particles/min, resulted in significant difference in dust concentrations while the interaction between the ventilation rate and the dust generation rate was not significant. The reasons that cause the disagreement between the measured values and those predicted by the model were discussed.

ACKNOWLEDGEMENTS

The author would like to express sincere thanks to everyone involved in the preparation of this thesis.

Special acknowledgement is due to:

- Dr. J. J. R. Feddes, for serving as supervisor and for guidance, advice and support throughout this study.

- Dr. J. Leonard and Dr. R. T. Hardin, for serving as committee members and for their suggestions concerning this study. Dr. Hardin's help with data analysis is also gratefully appreciated.

- Dr. C. M. Liao, for his invaluable assistance with the mathematical model.

TABLE OF CONTENTS

LIST OF TABLES

LIST OF FIGURES

LIST OF PLATES

LIST OF SYMBOLS

Symbol	Description	Units
[A]	diagonal matrix of lump's crossectional area	m^2
[B]	square transport matrix	min^{-1}
D(r)	molecular diffusion coefficient	cm^3/s
G(r,t)	dust generation rate	particles/s-μm
{G(t)}	vector of time-dependent dust generation rate	particles/min
H	height	m
[H]	diagonal matrix of lump's height	m
K(r,ρ)	collision frequency function	cm^3/sec
n(r,t)	dust concentration of particles with size r	particles/cm^3
n(t)	dust concentration at time t	particles/cm^3
{n(t)}	vector of dust particle concentration	particles/cm^3
$\bar{n}(\bar{t})$	dimensionless dust concentration	
$\bar{n}(s,s)$	dimensionless dust concentration at steady state condition	
Q	ventilation rate	m^3/hr
r	particle radius	μm
r_o	average particle radius	μm
S	wall surface area	m^2
[S]	diagonal matrix of lump's	

	surface area	m^2
t	time	s
$\bar{t}$	dimensionless time	
$U_s(r)$	particle terminal settling velocity	cm/s
V	volume	m^3
$[V]^{-1}$	inverse diagonal matrix of air volume	m^{-3}
β	entrainment ratio	dimensionless
δ	thickness of the concentration boundary layer	cm
ϵ	eddy diffusion coefficient	cm^3/s
ϵ_o	average energy dissipation rate	cm^2/s
ν	kinematic viscosity	cm^3/s
ρ	time-dependent particle radius	μm

INTRODUCTION

The adverse environment that can occur inside confinement units is one of the primary problems facing the swine production industry. Air quality control is an important aspect of environmental management of swine buildings. Air quality depends not only on moisture and concentrations of toxic gases and microorganisms, but also on the concentration of airborne dust. Dust, which consists of solid aerosols formed by mechanical disintegrations from a parent material, is one of the main aerial contaminants in livestock buildings. A large quantity of dust is produced in swine confinement buildings. Swine dust is a complex mixture of agents that have the potential to produce injury from direct irritation, toxic reaction, or allergic reaction (Donham et al., 1986). Airborne dust in swine shelters causes respiratory distress symptoms in both humans and pigs and may affect the growth rate of livestock. It causes deterioration of equipment such as ventilation ducts, fan motors, sensors, etc., in that they become less reliable or require servicing more frequently. Dust also is a carrier of odors. The odorous gases found to be associated with

airborne particles were identified as organic compounds of sulfur and ammonia (Bundy and Hazen, 1975).

Particles with a size of less than 5 microns (μm) can reach the lung tissue and are considered to be the most hazardous (Honey and McQuitty, 1979). The concentration of particles with sizes above the respirable range is also of importance (Heber et al., 1988) since the 5 - 20 μm diameter particles are primarily responsible for the odor-carrying ability of airborne dust (Honey and McQuitty, 1979; Burnett, 1969).

Dust in swine barns becomes airborne as a result of animal activity and air movement thus introducing finely ground dry feed during feeding and introducing fecal-feed particles deposited on a solid-floor. Although most dust particles tend to settle out, they can be continuously reintroduced into an airspace. Investigations show that the animal's activity has a strong influence on the dust concentration in the air. Dust concentration increases dramatically when animal activity is high (Gustafsson, 1989; Honey and McQuitty, 1979; McQuitty et al., 1985; Bundy and Hazen, 1974).

Airborne dust levels in swine buildings can be reduced by lowering the dust production rate by using methods such as pelletizing the feed, adding oil to the feed, introducing

a wet feeding system, encouraging less animal activity and restricting the duration of feeding or by using a dust collection device, etc.. Also, ventilation can be a primary mode for reducing airborne contaminants in animal housing. Contaminants can be diluted to safe levels by having a sufficient air exchange rate.

Much research work has been carried out in modelling and predicting the air contaminant concentration within a ventilated airspace. These studies have focussed on the macroscopic or microscopic features of airflow, such as airflow patterns, velocity profiles and contaminant dispersal within the space. They have used single or multi-cell, well- mixed models or numerical solutions to the microscopic changes of air and contaminant exchange in both agricultural and non-agricultural buildings. Behavioural models of aerosols in a ventilated airspace are of fundamental and practical significance because they not only provide useful information for the simulation of aerosols but, also, provide information for the design of removal mechanisms.

In a ventilated airspace, the time-dependent change in dust properties, such as particle size distribution and particle number and mass concentrations, can be determined by considering the simultaneous effects of coagulation, diffusion, deposition, thermopheresis, generation sources

and distribution of supplied air within the enclosure. Theoretical and experimental studies on this type of model have been presented by various researchers (Longstroth and Gillespie, 1947, Randolph and Larson, 1962; Huang et al., 1970; Greenfield et al., 1971; Lindauer and Castleman, 1971; Okuyama et al., 1976; Okuyama et al., 1980). Although approximate and semi-analytical sclutions for each effect and numerical solutions under particular conditions have been obtained, a general dynamic equation associated with the Navier-Stokes equation that describes a dust and airflow system in a ventilated airspace is extremely difficult to solve (Friedlander, 1977). The experimental results, on the other hand, were obtained under specific conditions and appeared insufficient to predict the general behavior under various conditions such as turbulent flow in a three-dimensional ventilated enclosure, or for different ventilation systems. The problem becomes more difficult for polydisperse particles and for ventilation systems with multiple inlets and outlets (Liao and Feddes, 1989).

Very little research work has been done to model air contaminant concentration distribution in livestock buildings. Choi et al. (1987) used the k-ϵ turbulent model to determine air contaminant concentration distribution in a ventilated airspace, but no attempt was made to validate the

predicted distribution. Dust behavior in a ventilated airspace has not been established satisfactorily for livestock buildings (Bundy and Hazen, 1975; Nilsson, 1982; Honey and McQuitty, 1979).

A general model was developed to understand the local transport phenomenon of airborne dust from the viewpoint of a lumped-parameter approximation for describing the dynamics of airborne dust at any location within a ventilated airspace (Liao and Feddes, 1990(b)). The governing equation of the lumped-parameter model is represented by a first-order, vector-matrix differential equation, or referred to as a linear dynamic equation.

An experiment was carried out in an environmental chamber to assess the accuracy of the model using talcum powder as a test dust (Liao and Feddes, 1990(a)) and the predictions of the model compared very favourably with the measured results. Talcum particles had an average aerodynamic diameter of 1 μm and their particle size distribution was quite uniform (Liao and Feddes, 1990(a)). In this study, the objective was to use the model to predict the concentrations of dust in an airspace using dust collected from a swine barn as the test dust. Both ventilation rate and dust generation rate were varied to test their effect on airborne dust concentration.

LITERATURE REVIEW

Dust in Swine Buildings

According to a comprehensive analysis of dust from swine houses (Donham et al., 1986), the main constituents of swine dust included animal feed components (starch granules, grain meal, trichomes, and corn silk) and swine fecal material (bacteria, gut epithelium, and undigested feed). Other identified components of the dust included swine dander, mold pollen, insect parts, and mineral ash. The relative proportion of feed to fecal content of the dust increased in buildings where larger animals were housed. The measured median diameter of the particles was about 2.2 μm. Most starch and grain meal particles had diameters larger than 5 μm, fecal material particles were between 1 and 2 μm diameter and among 11 to 16 μm diameter particles, about 1 and 10% were identified as hair and skin respectively (Heber et al., 1988(a)). Skin comprised 5% of the 7 to 9 μm particles (Honey and McQuitty, 1979). Both airborne and settled dust were primarily feed particles (Heber et al., 1988(a); Chiba et al., 1985; Curtis et al., 1975). Some researchers found that many large airborne particles were caused by electrostatic attraction between smaller particles (Koon et al.,

1963) and the attachment of viruses and bacteria (Harry, 1978; Dyment, 1976).

Airborne dust in pig finishing units was coarse and tannish and was more fluffy than dust from farrowing, nursery, and growing buildings because of higher quantities of feed used in the finishing units (Heber et al., 1988(a)). The respirable fraction was primarily fecal material, probably generated by animal movements (Donham et al., 1986).

Factors which may affect the dust concentrations in swine buildings are:

(1) temperature difference between inside and outside of the building (Heber et al., 1988(b)),

(2) the type of the ventilation system, i.e. natural ventilation system, or mechanical ventilation system (Phillips, 1986; Chiba et al., 1985; Heber et al., 1988(b)),

(3) air velocity (Harry, 1978; Bundy, 1984; Meyer and Manbeck, 1986),

(4) humidity (Honey and McQuitty, 1979; Bundy, 1984; Heber et al., 1988(b); Grub et al., 1965),

(5) animal activity was implicated as a major factor causing higher dust emissions and was associated with inside temperature (Koon et al., 1963; Honey and McQuitty, 1979); feeding methods (Honey and McQuitty, 1979; Bundy and Hazen, 1975); light compared to darkness in swine nursery and poul-

try housing (Van Wicklen and Yoder, 1988; Van Wicklen and Mitchell, 1986; Grub et al., 1965; McQuitty et al., 1985),

(6) the quantity of feed fed (Honey and McQuitty, 1979; Donham et al., 1986), and

(7) building hygiene (amount of dust and dry litter on the floor) (Mueller, 1984; Carpenter, 1986; Heber et al., 1988(b)).

Basic Concepts and Terminology

Factors affecting dust behavior

Dust particle size, concentration and chemical composition appear to be the main factors that affect human and animal health in livestock buildings. Particle size is the most important parameter for characterizing the behavior of aerosols. Most aerosols cover a wide range of sizes. Not only do aerosol properties depend on particle size but the relationships that govern their behavoir change with size. The sizes of particles influence their sedimentation rate (Janni et al., 1984) and the location of deposition in the respiratory tract (Mercer, 1978). Particles greater than 10 μm are deposited in the nasal passages, 5 - 10 μm in the upper respiratory tract and particles less than 5 μm reach lung tissue, and there appears to be no lower size limit for

deposition (Carpenter, 1

Coagulation

Coagulation of aerosols is a process whereby aerosol particles collide with one another due to a relative motion between them and adhere to form larger particles. The result of the coagulation is a continuous decrease in number concentration and an increase in particle size. Turbulent coagulation is caused by the turbulent motion of a flowing medium. Particles of different sizes move with different velocities and collide as a result. Generally, turbulent coagulation becomes very important for particles larger than 10 μm (Hinds, 1982) and the majority of dust particles found in animal housing have diameters between 0.5 and 5.0 μm (Van Wicklen et al., 1988). Therefore, the turbulent coagulation phenomenum is not significant compared to turbulent diffusive and gravitational deposition in an animal ventilated airspace.

Deposition by diffusion

A continuous diffusion of aerosol particles to a surface is due to a concentration gradient between the surface and its adjacent space. Particles deposit as a result of fluctuating velocities normal to the surface. Particles are

unable to follow the eddy motion and are projected to the wall through the relatively quiescent fluid near the surface. Diffusion decreases the concentration of dust particles as a result of the deposition of small particles on wall surfaces.

Gravitational Sedimentation

The particle motion is the result of gravity and the resistance of the gas to particle motion. Gravitational settling decreases the concentration as a result of deposition of larger particles on the floor.

Dust concentration

The most common measure of dust concentration is mass concentration: the mass of particulate matter in a unit volume of aerosol. Common units are g/m^3, mg/m^3, and $\mu g/m^3$.

Another common measure of concentration is number concentration: the number of particles per unit volume of aerosol. Common units are particle number/cm^3 and mppcf (million particles per cubic foot). Only number concentration expressed in particles/cm^3 is used in this study.

Air Space Distribution and Dust Concentration

A knowledge of airflow patterns in ventilated animal housing is important for control of contaminants such as harmful gases, dust, excessive heat, or water vapor, etc. since they are removed by ventilation only (Choi et al., 1987). The distribution of gases and dust pollutants in a ventilated enclosure depends not only on the characteristics of the pollutants themselves, and the ventilation airflow rates of clean air, but also on the flow field. The flow field in a ventilated enclosure is usually complex. It can be defined in terms of supplied airflow, pollutants flow, infiltration flow, and recirculation airflow, etc.. Furthermore, turbulent flow is a typical feature of the airflow in a ventilated enclosure (Liao, 1989). Air velocity fields must be determined if air quality is to be predicted analytically (Choi et al., 1987).

Substantial research work has been carried out in predicting airflow patterns in an ventilated enclosure (Timmons et al., 1980; Nielsen, 1973; Nielsen et al., 1978; Gosman et al., 1980; Choi et al., 1987, 1988; Randall, 1977).

Some general rules suggested by Randall (1977), and Randall and Battams (1979) predict qualitatively the airflow pattern in a ventilated livestock building. They were as

follow:

1) Primary air paths are established from the inlet to the outlet in the directions of airflow.

2) Air moves in a series of rotary motions.

3) Secondary paths are induced by the primary paths to complete one or more rotary motions.

According to the studies of Randall (1977, 1980), Randall and Battams (1976) and Boon (1978), the initial velocity of the inlet air, ceiling obstructions, the layout of pens and design of partition structures within the building, exert a great influence on the airflow patterns within the building. The air space distribution also depends on whether the incoming air is used for heating or cooling.

By examining the air distribution patterns it has been shown that the air space can be roughly divided as follows (ASHRAE, 1989):

1. The primary air zone. This is an air envelope developed from the air inlet to where the air velocity approaches 0.75 m/s.

2. The total air zone. This zone includes the primary air zone and the entrained air from the general air motion zone. The air velocity in this zone is relatively high as it is influenced by the primary air, but less than 0.75 m/s.

3. The stagnant zone. This zone results from natural

convection currents. Air velocity within this zone is usually low (approximately 0.1 m/s).

4. The general building air motion zone. This is the part of space in which there is a gentle drift towards the total air zone, i.e., entrainment. Air motion in this space is attributed to the recycling of total air.

An example of typical airflow pattern in a ventilated enclosure was given by Liao (1989) and is shown schematically in Figure 1. In this example, inlets are mounted in or near the ceiling and discharge air horizontally. In the side view (Figure 2), "A" denotes the volume space which is composed of primary air and the total air zones, and "B" denotes the space or volume which corresponds to the general building air motion zone. Below zone "B" is the stagnant zone. According to Barber and Ogilvie's studies (1982), completely stagnant zones are unlikely to exist in livestock buildings, and the multiple flow regions were considered to be the most likely reason for departures from complete mixing which was normally assumed in designing of livestock building ventilation systems in slot-ventilated airspace.

Airflow patterns in a ventilated airspace will definitely affect the concentration distributions of aerial contaminants such as gaseous pollutants and dust (Liao, 1989; Choi et al., 1987; De Praetere and Van Der Biest, 1989;

Robertson, 1989; Heber et al., 1988(b); Brannigan and McQuitty, 1971). Therefore, the accurate prediction of air flow patterns and velocity profiles are essential for better prediction of contaminant concentration distribution. On the other hand, the contaminant concentration distributions can be a direct measure of effectiveness of ventilation in achieving acceptable air quality in a ventilated livestock building.

The Population-Balance Equation

The population-balance equation (from a micro-mixing point of view, Himmelblau and Bischoff, 1968) can be termed a General Dynamic Equation (GDE) and is the basic equation for such a system describing the time-dependent change in properties of an airborne dust undergoing turbulent coagulation, turbulent diffusive deposition, gravitational settling, and ventilation airflow. Such an equation can be written as (Friedlander, 1977; Davies, 1966; Greenfield et al., 1971; Okuyama and Kousaka, 1977; Liao and Feddes, 1989):

$$\partial n(r,t)/\partial t = 1/2\int_{\rho=0}^{\rho=r/2^{1/3}} K((r^3-\rho^3)^{1/3},\rho)n((r^3-\rho^3)^{1/3},t)$$

$$n(\rho,t)(r/(r^3-\rho^3)^{1/3})^2 d\rho$$

$$-\int_0^\infty K(r,\rho)n(r,t)n(\rho,t)d\rho$$

$$-(D(r)+\epsilon)S/(\delta V)n(r,t)$$

$$-U_s(r)/Hn(r,t)-Q/Vn(r,t)+G(r,t)/V \qquad (1)$$

and

$$G(r,t) = Qn_i(r,t) \qquad (2)$$

where:

G(r,t) = dust generation rate, particles/s/μm

Q = volumetric airflow rate, m^3/min, and

$n_i(r,t)$ = time-dependent initial concentration of dust at certain particle radius r, particles/cm^3/μm

The left side of equation (1) indicates the change in particle number concentration of particles with size r at time t. The first term on the right hand side represents the rate of formation of particles of size r due to turbulent coagulation of two particles smaller than r, and the second term the rate of loss of particles of size r due to their coagulation with particles of any other sizes including r. The third term indicates the rate of deposition by turbulent diffusion and the fourth term the rate of

deposition by gravitational sedimentation. The fifth term represents the rate of particles removed from a system volume by ventilation airflow and the sixth term indicates the rate of particle generation in a system volume.

Equation (1) was derived on the basis of several assumptions (Appendix A). It is a nonlinear partial integro-differential equation and cannot be solved analytically. By simplification and further assumptions, a linear ordinary differential equation was derived (Liao and Feddes, 1989):

$$dn(t)/dt = -5.2r_o^3(\epsilon_o/\nu)^{1/2}n^2(t) - U'_s(r_o)/Hn(t) - (D(r_o)+\epsilon)S/(\delta V)n(t) + Q/V(n_i - n(t)) \qquad (3)$$

This model was relatively primitive since it assumed the system interior to be a single, well-mixed volume, and did not account for the spatial changes in physical dynamics of the interior environment.

The Lumped-Parameter Model

The lumped-parameter model was derived based on the linear ordinary differential equation (Liao and Feddes, 1990). The extended developments to the linear ordinary differential equation included:

(1) multivolumes, based on lumped-parameter approximation,

(2) a model for predicting dust particle concentrations that incorporates a description of local transport phenomena characterized by local airflow rates and transition probabilities of airborne dust particles.

As shown in Figure 3, a ventilated airspace can be divided into m arbitrary lumps. In each lump, the mixing is assumed to be uniform and instantaneous, and concentration is constant throughout the lump. The particle concentration change with time in each lump can be represented as the sum of two terms. The first term that represents processes which occur inside the lump may include gas-to-particle conversion and turbulent coagulation. The second term indicates particle transport across the boundaries of the lump by transfer airflow rates, turbulent diffusion, and gravitational sedimentation.

With the model assumption (Appendix B) and the linear ordinary differential equation, by applying the advanced matrix method, the system equation can be represented by a first-order vector-matrix differential equation:

$$d\{n(t)\}/dt = -[B]\{n(t)\} + [V]^{-1}\{G(t)\}, \quad \{n(0)\} = \{n_o\} \qquad (4)$$

where:

$\{n(t)\}$ = vector of dust particle concentration, particles/cm^3

$[V]^{-1}$ = inverse diagonal matrix of air volume, m^{-3}

$\{G(t)\}$ = vector of time-dependent dust generation rate, particles/min,

$[B]$ = square transport matrix, min^{-1}, and

$\{n_0\}$ = vector of initial airborne dust concentration, particles/cm^3.

The transport matrix [B] also can be expressed as:

$$[B]=[H']^{-1}+[V]^{-1}[S']+[T]^{-1} \qquad (5)$$

where:

$$[H]^{-1}=[V]^{-1}[A]$$

$$[H']^{-1}=U_s(r)[H]^{-1}$$

$$[T]^{-1}=[V]^{-1}[Q], \text{ and}$$

$$[S']=((D(r)+\epsilon)/\delta)[S]$$

in which:

[A] = diagonal matrix of lump cross-sectional areas, m^2

[H] = diagonal matrix of lump heights, m

[S] = diagonal matrix of lump surface areas, m^2

Us(r) = particle terminal settling velocity, cm/sec

D(r) + ϵ = effective turbulent diffusion coefficient, cm^2/sec, and

δ = thickness of concentration boundary layer, mm.

[Q] is a square airflow matrix with components Qij, where:

$$Q_{ij} = \begin{cases} -Q_{ij} & for \quad i \neq j \\ \sum_{\substack{i=1 \\ (i \neq k)}}^{m} Q_{ki} & for \quad i = j \end{cases} \qquad (6)$$

For the i^{th} row of [Q] the off-diagonal entries represent the airflow rates into the i^{th} lump from other lumps with negative sign, while the diagonal entries give the total airflow out of the i^{th} lump. The airflow matrix [Q] also can be expressed as :

$$[Q] = Q[\beta] \qquad (7)$$

where:

[β] = square matrix of entrainment ratio function,

Q = total volumetric flow rate of outdoor air supplied to the whole system, m^3/hr.

The equilibrium dust particle concentrations attained can be given as:

$$\{n(s,s)\} = [B]^{-1}[V]^{-1}\{G(s,s)\} \qquad (8)$$

where:

{G(s,s)} = vector of equilibrium dust generation rate, particles/min.

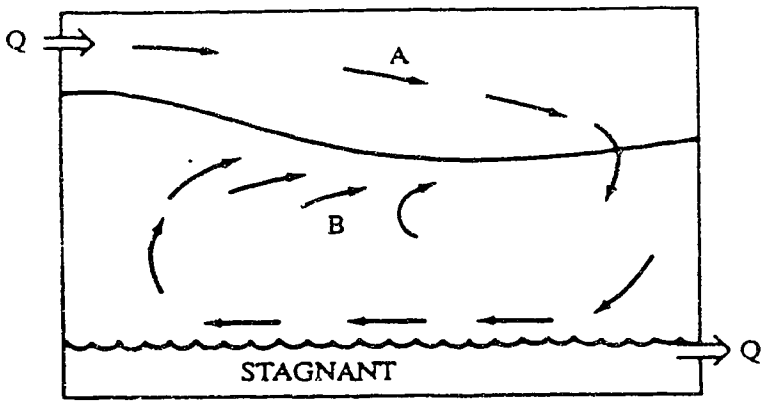

FIGURE 1. Schematic diagram of a typical airflow pattern in a ventilated enclosure (Liao, 1989)

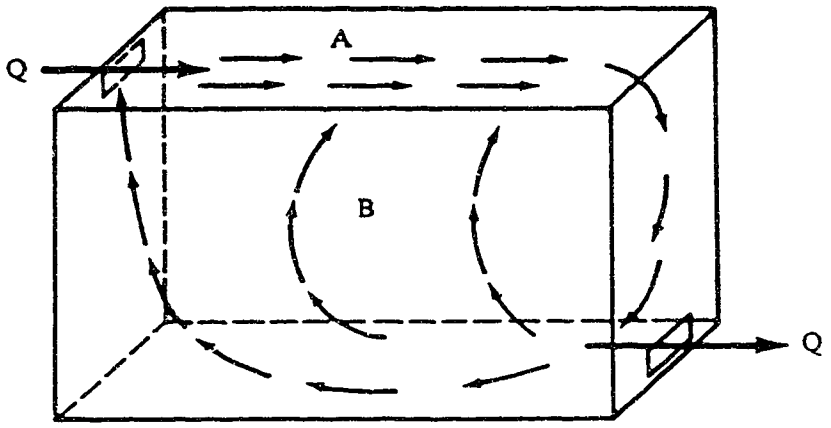

FIGURE 2. Typical air flow pattern in a ventilated enclosure (side view) (Liao, 1989)

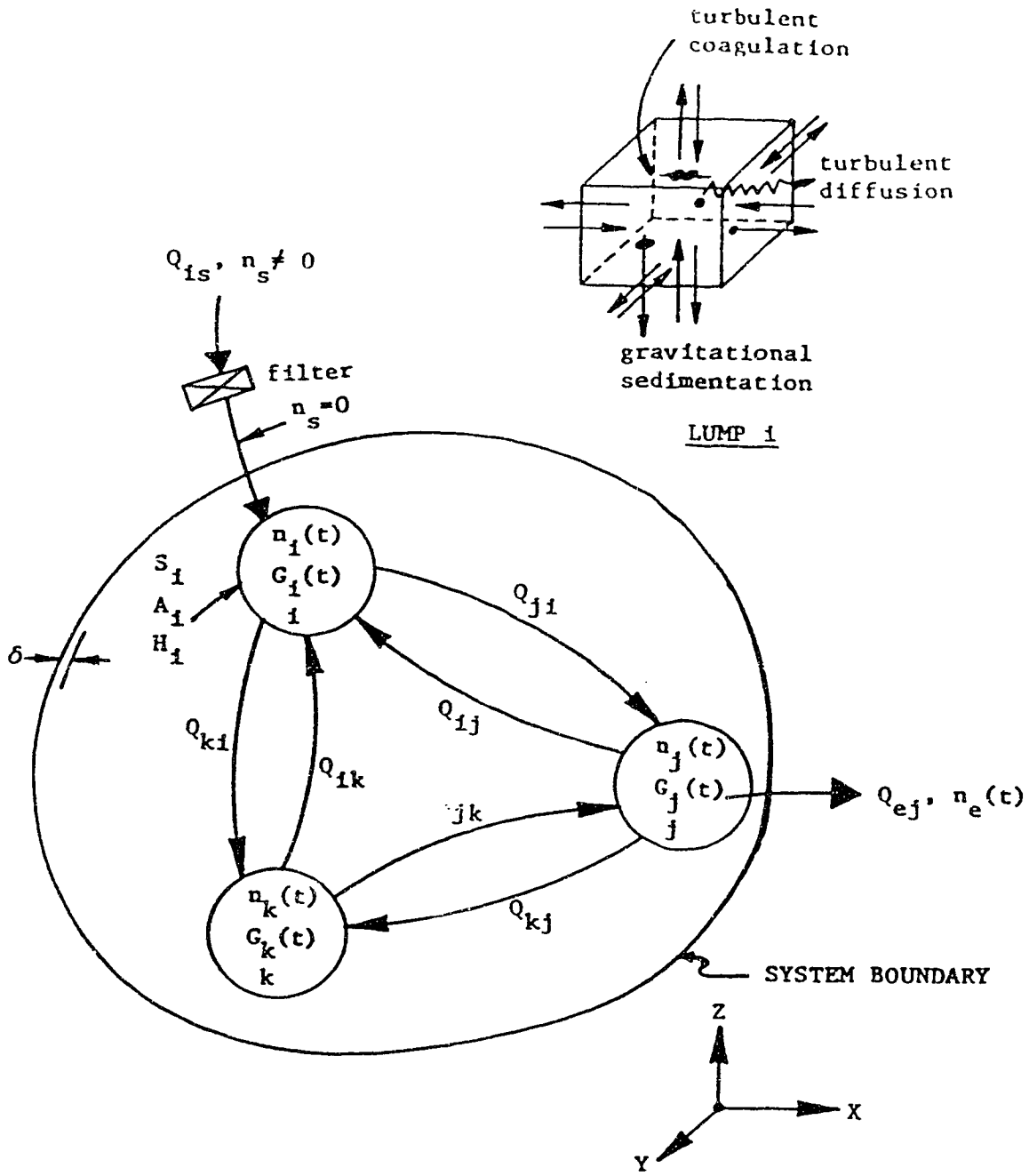

FIGURE 3. Schematic diagram of a lumped-parameter model and a control volume i of ventilation airborne dust systems (Liao and Feddes, 1990(a))

EXPERIMENTAL PROCEDURE

Experimental Facility and Test Dust

Environmental chamber

The experiment was carried out in an experimental chamber which was constructed within a controlled-environmental building (Leonard, 1986) at the Agricultural Engineering Research Station, Ellerslie, Alberta. The chamber, which was designed to simulate a small room housing pigs, has dimensions of 7.2m x 5.4m x 1.9m with a volume of 74 m^3. The major dimensions are indicated on the overall view of the chamber shown in Figure 4.

Ventilation system

Air entered the test chamber from the air-conditioned building through an inlet (5400x45 mm) (Figure 5). A 640 mm diameter, 7-blade propeller fan (Model ECDQ 562/6, Zeihl - Abegg Co.) was used to exhaust air from the chamber. The height of the fan centreline was 1 m above the floor. The fan speed control was achieved with a controller (Model MC - 5C, Tri Var Inc., Mississauga, ON) to maintain constant air-flow rates over the sampling period (Figure 5). The fan operating capacities were 0 to 1500 m^3/hr. The airflow rate

was measured near the end of the discharge duct in accordance with Jorgenson (1983). Three ventilation rates 300, 900, and 1500 m^3/hr were chosen to simulate the cold and warm weather ventilation rates in an animal building.

Test Dust

The dust used throughout the experiment was collected from a pen floor in a feeder swine barn. The collected dust was sieved through a screen with 4.76 mm (Mesh No. 4) openings to remove the larger material. In order to obtain a homogeneous dust, the screened dust was mixed in a rolling cylinder for one hour.

Dust generation system

The dust was placed in a hopper and transported by an auger to a blower that injected it into the ventilated airspace at six dust generation locations (Figure 6). The dust generating points were 27 cm above the floor. The generation rate was changed by installing augers with different pitches. Three augers were fabricated to meet the requirement for dust generation rates (Plate 1).

Instrumentation

A TSI-APS 3300 Aerodynamic Particle Sizer System (TSI, St. Paul, MN) was used to measure dust particle concentration (Plate 2). Before the test, the APS was calibrated with known particles of Uniform Latex Polystyrene Microspheres (0.496, 0.966, 2.01 μm), Styrene-Vinytoluene Latex Polymer Microspheres (2.96 μm), and Polymer Microspheres (3.983, 9.870 μm) (Duck Scientific Corp., Palo Alto, CA).

The Model 3460 Tri-Jet Aerosol Generator (TSI, St. Paul, MN) was used to produce aerosols from liquid solutions and suspensions to calibrate the APS (Plate 3).

As shown in Plate 4, the velocity of airflow rate in the duct downstream from the ventilation fan was measured by an airflow meter (Velocicalc, Model 8350, TSI Incorporated, St. Paul, MN).

Airborne dust concentration sampling

A total of 12 sampling points detected concentrations in both longitudinal and vertical directions. Sampling was carried out in two planes, 1.8 m and 3.6 m from a side wall (along y-direction in Figure 5). To calculate dust generation rates, the airflow rates and dust particle concentrations generated from the six dust generation points were

measured before each experiment. Dust samples were drawn to the particle sizer via a 1.3 cm internal diameter Tygon plastic tubing at a rate of 16.67 cm^3/s. At this airflow rate, the dust particle velocity is sufficient to prevent particles settling in the sampling tubes. Sampling point 5 was used to study the transient responses of airborne dust at a sampling interval of 2 minutes (Figure 5). Equilibrium was assumed to occur 60-70 minutes after a constant dust concentration was reached in the exhaust air. After 100 minutes, concentrations at 12 sampling points were measured in a random order. The environmental chamber was cleaned before each trial run. Sampling tubes were cleaned by compressed air before sampling.

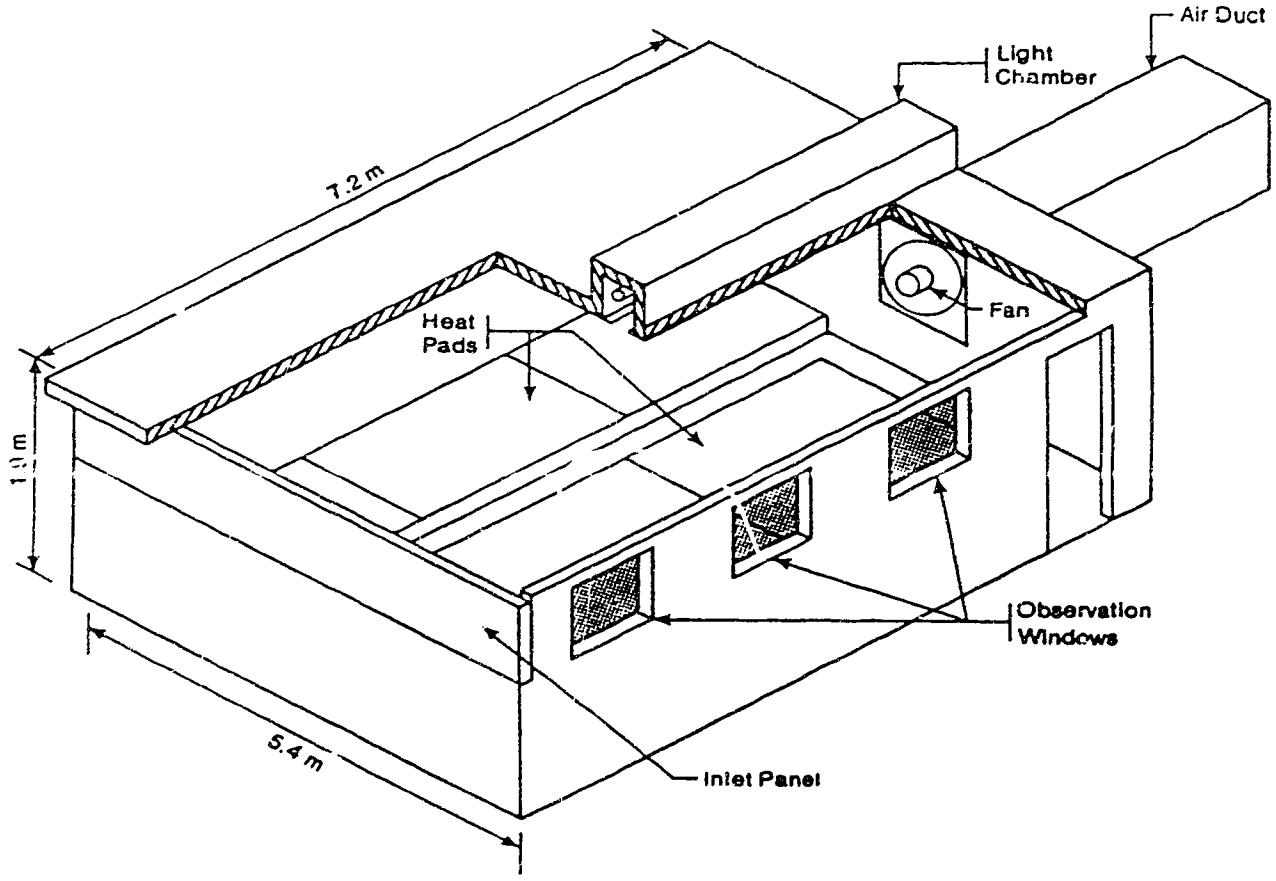

FIGURE 4. Overall view of large-size environmental chamber (Leonard, 1986)

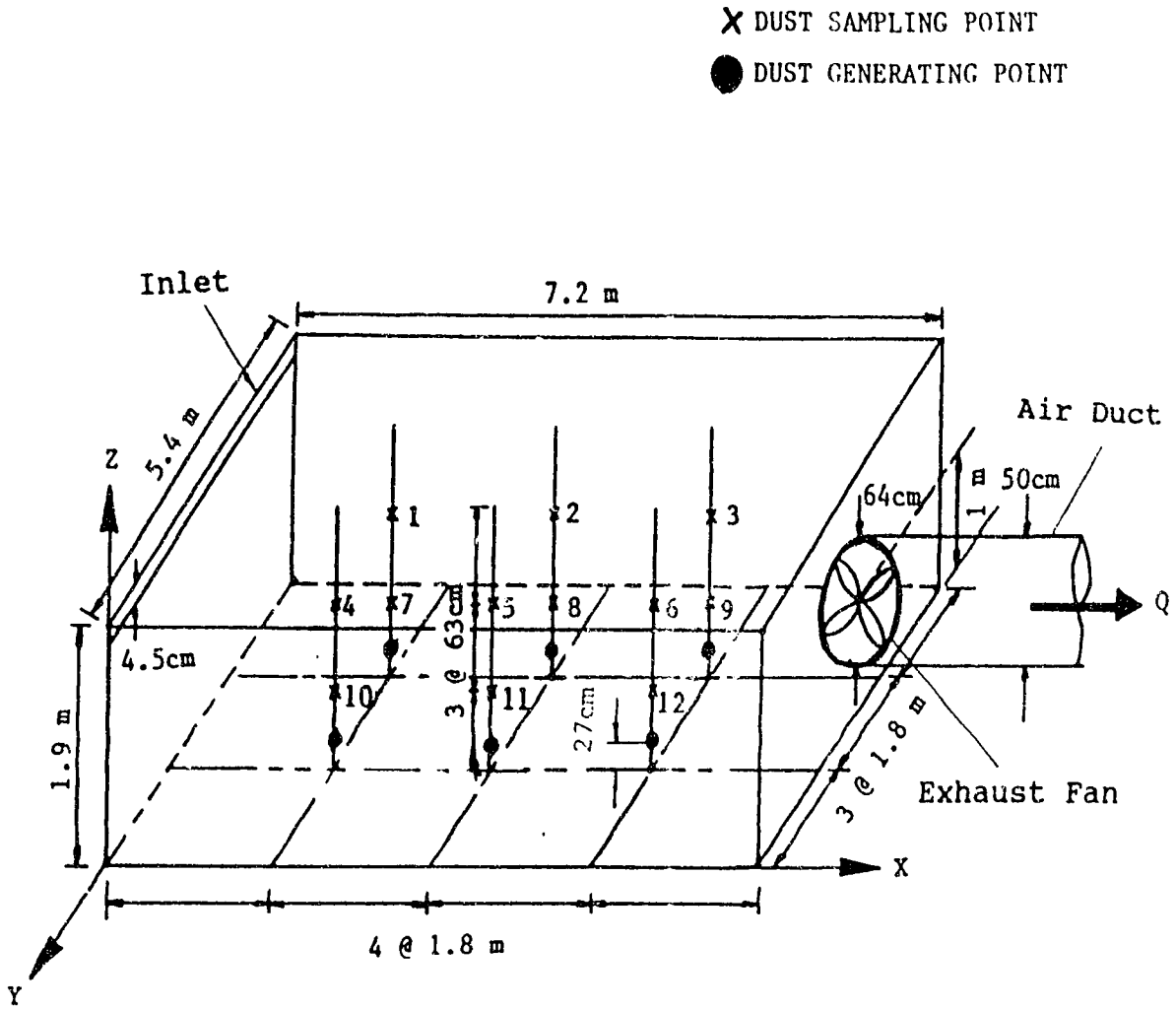

FIGURE 5. A general outline of the environmental chamber showing the locations of sampling and dust generating point

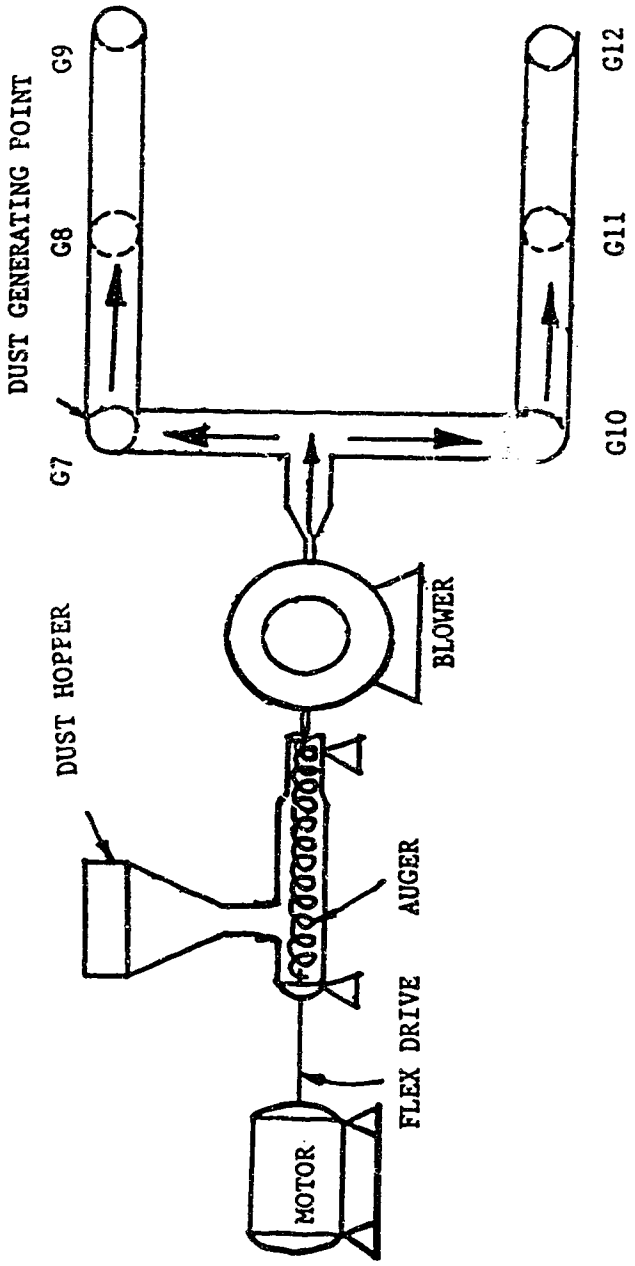

FIGURE 6. General outline of dust generating system

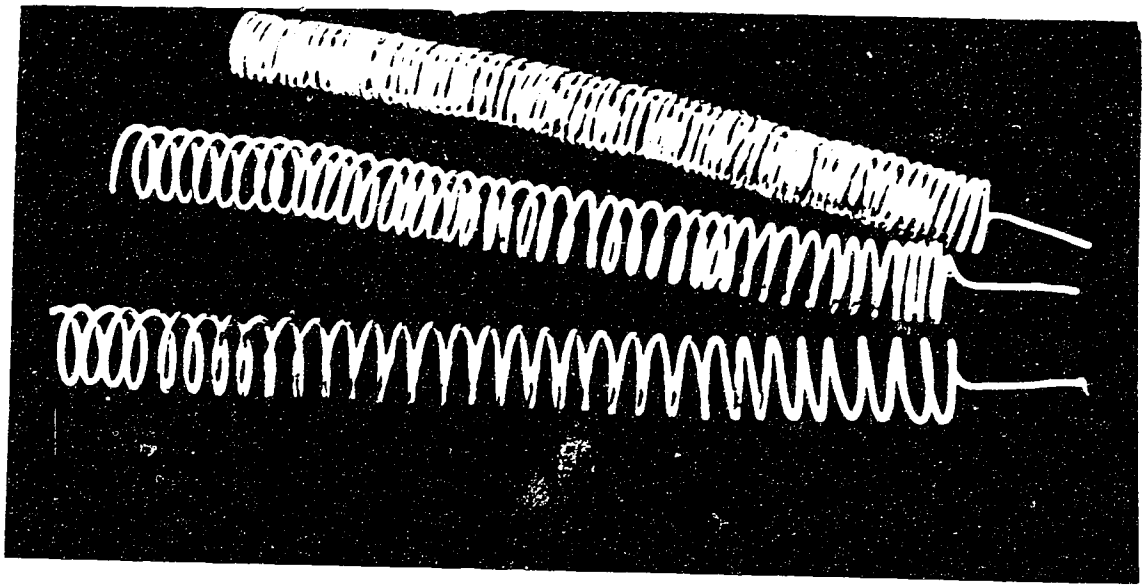

PLATE 1. Augers used to provide different dust generation rates.

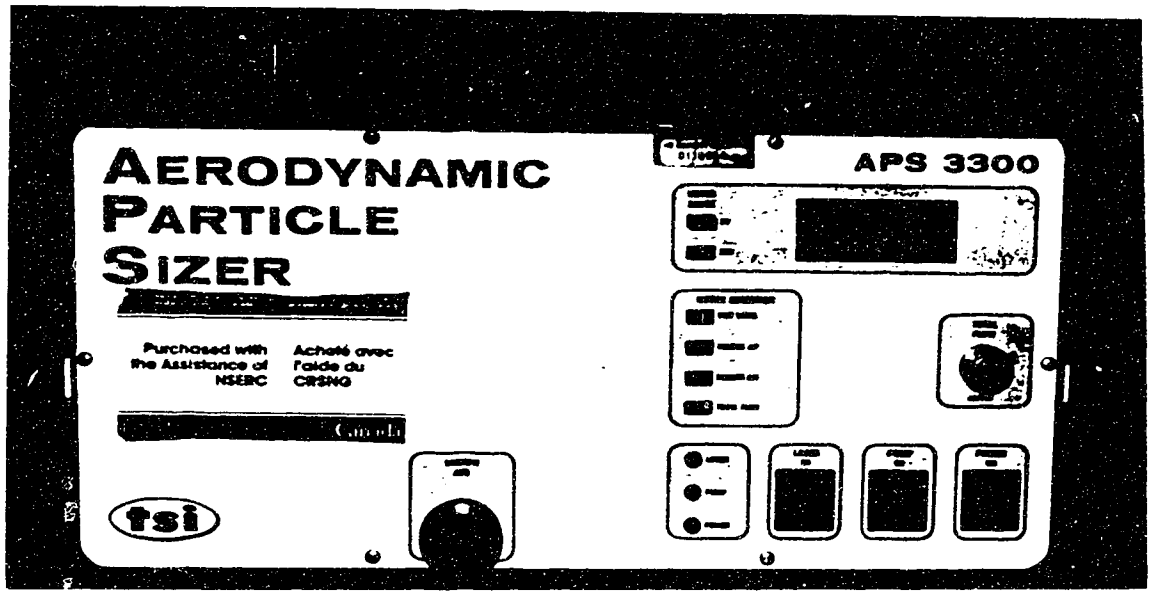

PLATE 2. TSI-APS 3300 Aerodynamic Particle Sizer.

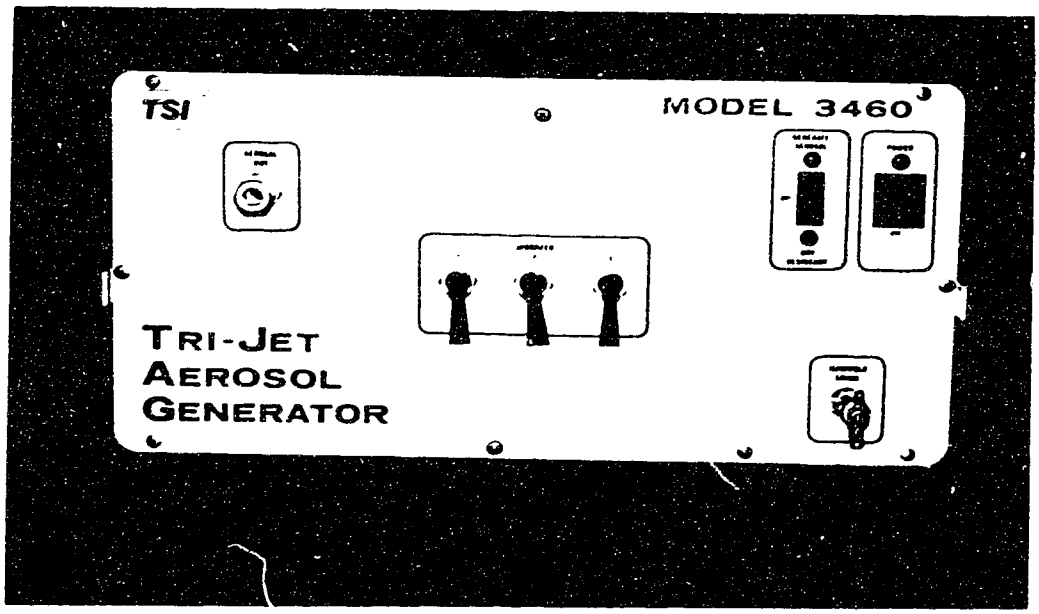

PLATE 3. Model 3460 Tri-Jet Aerosol Generator.

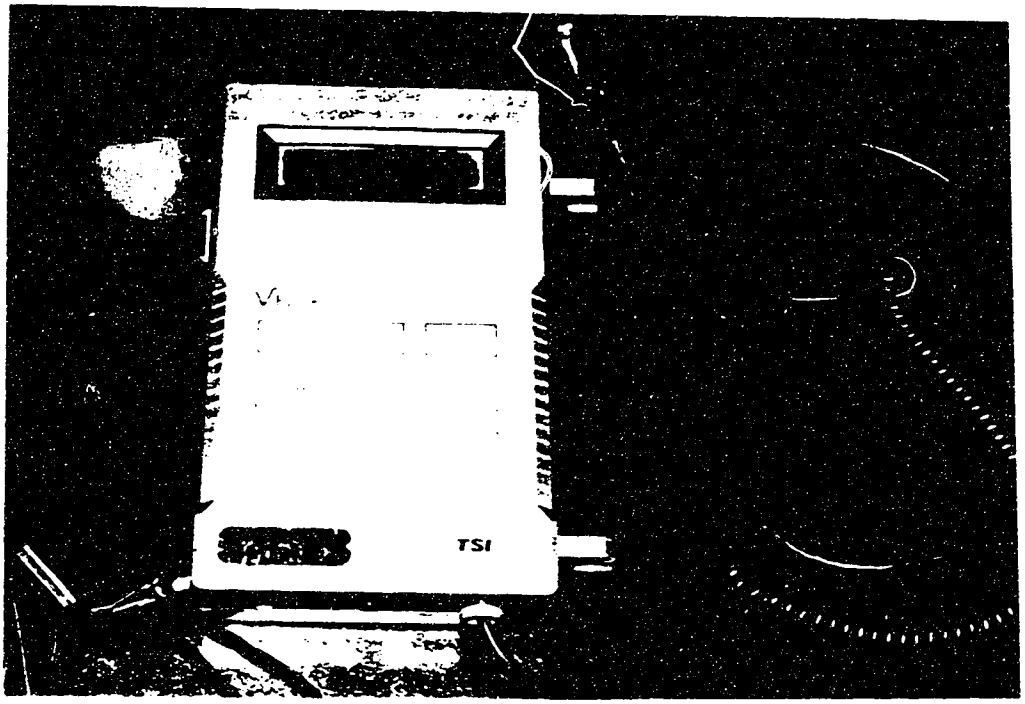

PLATE 4. Air velocity meter (Model 8350, Velocicalc).

METHODOLOGY

Experimental Design

The primary dependent factor studied in this project was the airborne dust concentration. Independent factors consisted of three levels of ventilation rates (300, 900, 1500 m^3/hr) and three levels of dust generation rates ($533x10^6$, $554x10^6$, $665x10^6$ particles/min). The two independent factors, each having three levels, yielded a total of 9 possible combinations. The 9 possible combinations are listed in Table 1. Each combination was replicated three times in a random order. These were arranged in a split-split-plot factorial experimental design so that the dust concentration data could be analyzed using an analysis of variance procedure. The statistic model of the experiment is:

$$C = \mu + V_i + D_j + VD_{ij} + R_{k(ij)} + L_l + LV_{il} + LD_{jl} + LVD_{ijl} + LR_{kl(ij)} + S_m + SV_{im}$$
$$SD_{jm} + SVD_{ijm} + SL_{lm} + SLV_{ilm} + SLD_{jlm} + SLVD_{ijlm} + \epsilon_{ijklm} \qquad (9)$$

where:

μ = overall mean

V_i = ventilation airflow rates i = 1, 2, 3

D_j = dust generation rates $j = 1, 2, 3$

R_k = replicates $k = 1, 2, 3$, and

L_l = levels $l = 1, 2$

S_m = lumps $m = 1, 2, \ldots 6$

As shown in the EMS table (Appendix C), the valid error term for testing the significance of ventilation rates and dust generation rates is the REPLICATES within the combination. The statistical analysis was performed using the GLM procedure of SAS (SAS Institute Inc., 1989).

Table 1. Possible combinations for the experiment

Dust Generation Rate	Ventilation Rate (m^3/hr)		
g (10^6 particles/min)	V_1 (300)	V_2 (900)	V_3 (1500)
g_1 (553)	g_1V_1	g_1V_2	g_1V_3
g_2 (554)	g_2V_1	g_2V_2	g_2V_3
g_3 (665)	g_3V_1	g_3V_2	g_3V_3

Verification of the Lumped-Parameter Model

As shown in the Figure 7, the environmental chamber was divided into 12 lumped control volumes in the x-y-z coordinates. The control volume P in the Figure 7 is a typical 3-D lumped volume in the system in which its representative

dust particles are undergoing turbulent diffusive deposition, gravitational sedimentation, and local airflow transport. The primary airflow and circulating airflow are assumed to be directed in the x, y, and z directions (Liao and F ldes, 1990).

The procedures of the model verification include:

1. From equations (4), (7), and (8), the following information is required for the model calculation:

a) The entrainment ratio, β: The actual value of the entrainment ratio depends upon the relative position between the supply and the exhaust position, size and shape (circular or slot, etc.) of the nozzle or air jet. In the model calculation, the secondary airflow rate (βQ) in a ventilated enclosure is assumed to be entirely induced by the primary airflow rate, i.e., the surrounding air is entrained into the inlet jet to become part of it.

The equation for the air entrainment in a jet stream from a long continuous slot has been mathematically presented in ASHRAE (1989):

$$\beta = \beta Q/Q = \textit{entrained flow/initial flow}$$

$$= \sqrt{(2/K')(X/H_o)} \qquad (10)$$

where:

K' = proportionality constant, approximate value of 7,

X = distance from inlet, m, and

H_o = width of slot, m.

In this model verification, air entered the experimental chamber through the 540x4.5 cm long slot. Therefore, the values for K', X, and Ho are 7, 7.2 m, and 4.5 cm, respectively. Substituting all these values into equation (10), the value of β is equal to 6.76.

b) The diagonal air volume matrix [V]: An equal air volume for all lumps is assumed in the model verification, i.e. $V_1 = V_2 = V_3 = \ldots\ldots V_{12} = 74/12\ m^3 = 6.16\ m^3$.

c) The steady-state dust generation rate {G(s,s)}: Dust generation occurred in lumps 7, 8, 9, 10, 11, and 12 (Figure 7). Dust concentrations at the six dust generation points were converted to dust generation rates in particles/min by multiplying the particle concentration by the airflow rate in each genration tube. The values of dust generation rate in the six lumps were denoted by G_7, G_8, G_9, G_{10}, G_{11}, and G_{12}, respectively. The airflow rates and the dust generation rates of the six dust generating points were listed in Table 2.

Table 2. Measured airflow and dust generation rates at the six dust generating points

dust generating point	airflow rate m^3/hr	dust generation rate (10^6 particles/min) low	medium	high
G_7	16.6	67.2	47.8	114
G_8	12.5	45.8	76.9	101
G_9	10.4	23.5	50.2	61.3
G_{10}	26.3	136	143	185
G_{11}	21.6	184	117	111
G_{12}	22.0	77.0	119	93.8
Total		533	554	665

d) The airflow matrix [Q]: From equation (6) and (7),and the airflow patterns that are shown schematically in Figure 8, [Q] can be expressed as:

$$[Q] = \begin{pmatrix} Q_{11} & -Q_{12} & -Q_{13} & -Q_{14} & \cdots & -Q_{1n} \\ -Q_{21} & Q_{22} & -Q_{23} & -Q_{24} & \cdots & -Q_{2n} \\ -Q_{31} & -Q_{32} & Q_{33} & -Q_{34} & \cdots & -Q_{3n} \\ -Q_{41} & -Q_{42} & -Q_{43} & Q_{44} & \cdots & -Q_{4n} \\ \cdot & \cdot & \cdot & \cdot & \cdot & \cdot \\ \cdot & \cdot & \cdot & \cdot & \cdot & \cdot \\ \cdot & \cdot & \cdot & \cdot & \cdot & \cdot \\ -Q_{m1} & -Q_{m2} & -Q_{m3} & -Q_{m4} & \cdots & Q_{mn} \end{pmatrix}$$

$$= Q[\beta]$$

$$= Q \begin{pmatrix} 1/2+3/2B & -1/2B & 0 & -1/2B & 0 & 0 & -1/2B & 0 & 0 & 0 & 0 & 0 \\ -1/2-1/2B & 1/2+2B & -1/2B & 0 & -1/2B & 0 & 0 & -1/2B & 0 & 0 & 0 & 0 \\ 0 & -1/2-1/2B & 1/2+3/2B & 0 & 0 & -1/2B & 0 & 0 & -1/2B & 0 & 0 & 0 \\ -1/2B & 0 & 0 & 3+3/2B & -1/2B & 0 & 0 & 0 & 0 & -1/2B & 0 & 0 \\ 0 & -1/2B & 0 & -1/2-1/2B & 1/2+2B & -1/2B & 0 & 0 & 0 & 0 & -1/2B & 0 \\ 0 & 0 & -1/2B & 0 & -1/2-1/2B & 1/2+3/2B & 0 & 0 & 0 & 0 & 0 & -1/2B \\ -1/2B & 0 & 0 & 0 & 0 & 0 & 3/2B & -1/2B & 0 & -1/2B & 0 & 0 \\ 0 & -1/2B & 0 & 0 & 0 & 0 & -1/2B & 2B & -1/2B & 0 & -1/2B & 0 \\ 0 & 0 & -1/4-1/2B & 0 & 0 & 0 & 0 & -1/2B & 1/4+3/2B & 0 & 0 & -1/2B \\ 0 & 0 & 0 & -1/2B & 0 & 0 & -1/2B & 0 & 0 & 3/2B & -1/2B & 0 \\ 0 & 0 & 0 & 0 & -1/2B & 0 & 0 & -1/2B & 0 & -1/2B & 2B & -1/2B \\ 0 & 0 & 0 & 0 & 0 & -1/4-1/2B & 0 & 0 & -1/2B & 0 & -1/2B & 1/4+3/2B \end{pmatrix}$$

$$= Q \begin{pmatrix} 10.64 & -3.38 & 0 & -3.38 & 0 & 0 & -3.38 & 0 & 0 & 0 & 0 & 0 \\ -3.88 & 14.02 & -3.88 & 0 & -3.88 & 0 & 0 & -3.38 & 0 & 0 & 0 & 0 \\ 0 & -3.88 & 10.64 & 0 & 0 & -3.38 & 0 & 0 & -3.38 & 0 & 0 & 0 \\ -3.38 & 0 & 0 & 10.64 & -3.38 & 0 & 0 & 0 & 0 & -3.38 & 0 & 0 \\ 0 & -3.38 & 0 & -3.88 & 14.02 & -3.38 & 0 & 0 & 0 & 0 & -3.38 & 0 \\ 0 & 0 & -3.38 & 0 & -3.88 & 10.64 & 0 & 0 & 0 & 0 & 0 & -3.38 \\ -3.38 & 0 & 0 & 0 & 0 & 0 & 10.64 & -3.38 & 0 & -3.38 & 0 & 0 \\ 0 & -3.38 & 0 & 0 & 0 & 0 & -3.38 & 13.52 & -3.38 & 0 & -3.38 & 0 \\ 0 & 0 & -3.63 & 0 & 0 & 0 & 0 & -3.38 & 10.39 & 0 & 0 & -3.38 \\ 0 & 0 & 0 & -3.38 & 0 & 0 & -3.38 & 0 & 0 & 10.14 & -3.38 & 0 \\ 0 & 0 & 0 & 0 & -3.38 & 0 & 0 & -3.38 & 0 & -3.38 & 13.52 & -3.38 \\ 0 & 0 & 0 & 0 & 0 & -3.63 & 0 & 0 & -3.38 & 0 & -3.38 & 10.39 \end{pmatrix} \quad (m^3/min)$$

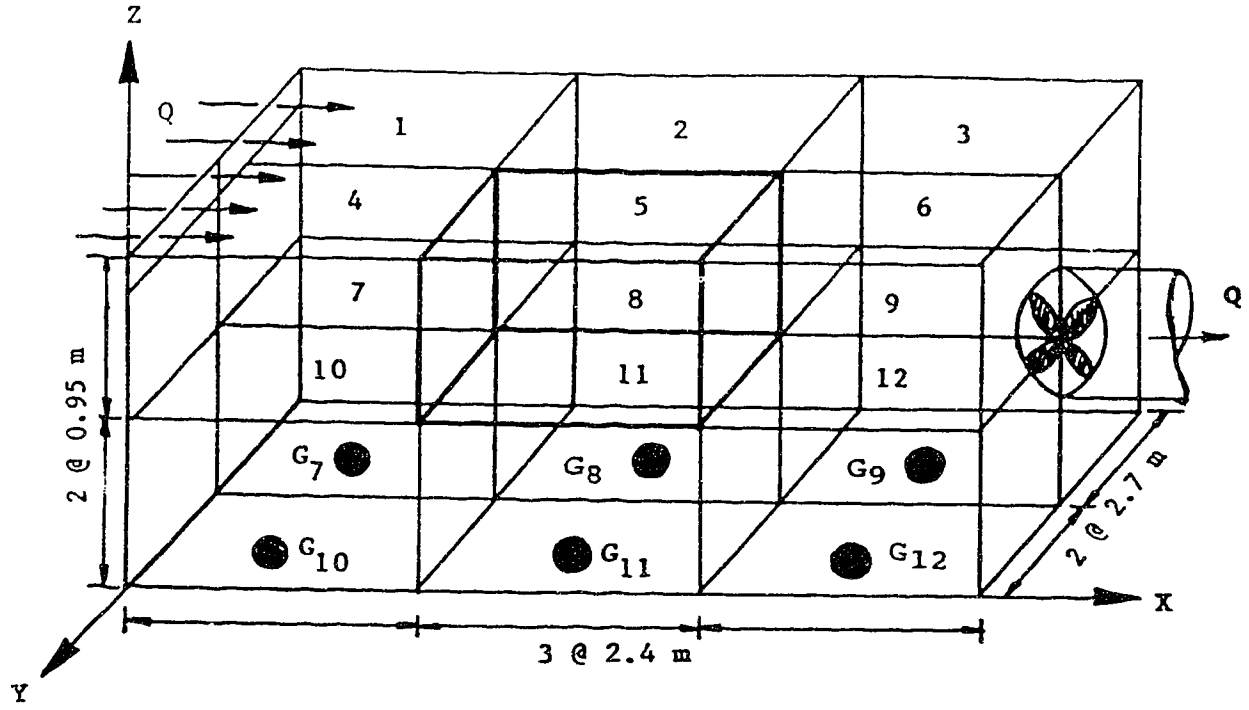

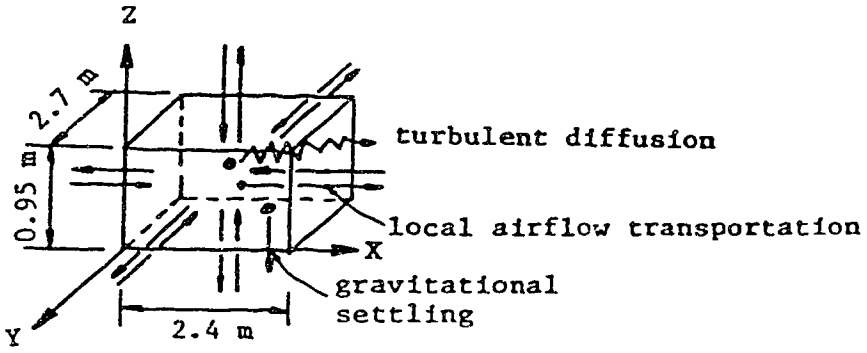

CONTROL VOLUME P

FIGURE 7. Twelve lumps and a control volume P used in the model verification

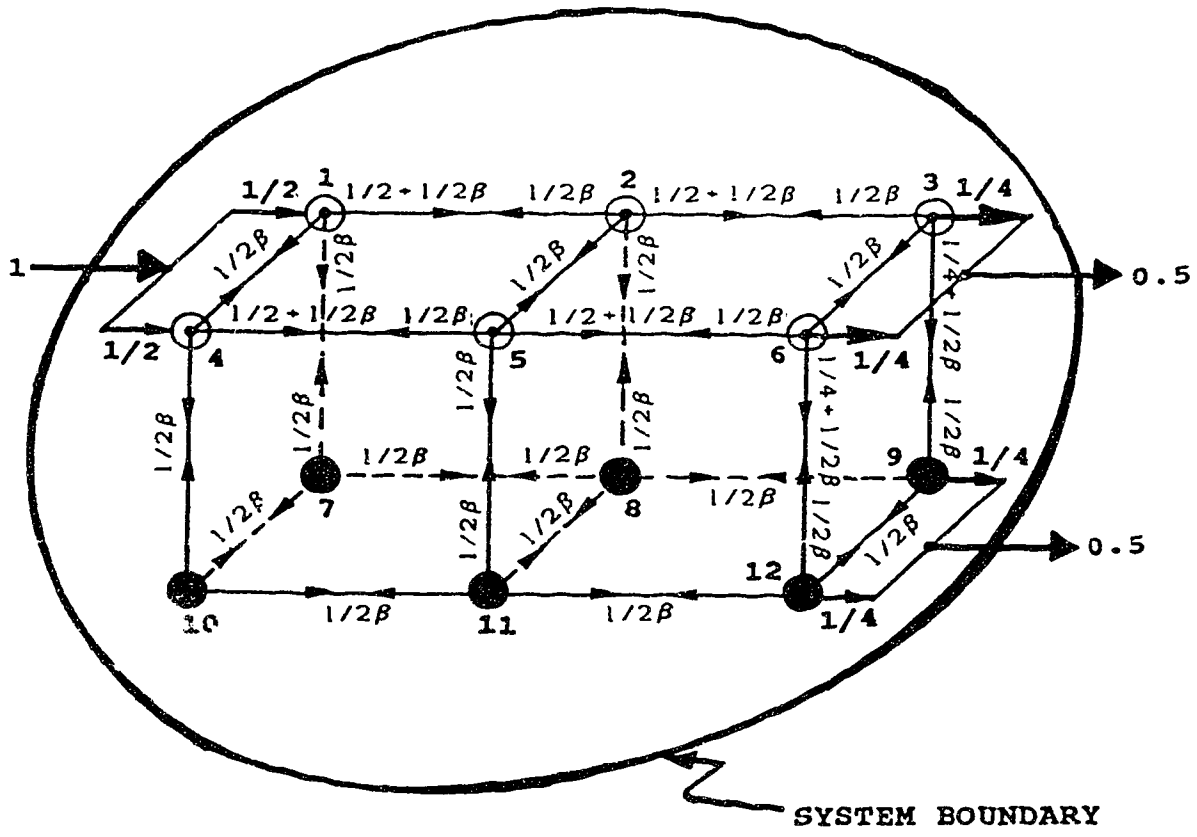

FIGURE 8. Airflow patterns of a 12-lump model used in model verification

The airflow matrix is quasi-diagonally dominant, i.e., the diagonal element of airflow matrix, in row i or in column i, Qii, is larger than or equal to its corresponding column sum or row sum. Figure 8 indicates that the solution of the airflow matrix is by the 3-D lumped form of control volumes represented by the conservation of airflow rates.

e) The transport matrix [B]: The input data of the transport matrix are determined by equation (5). The particle terminal settling velocity is assumed as Us(r) = 0.013 cm/sec (Hinds, 1982), effective diffusion coefficient as $D(r)+\epsilon = 3.34\times10^{-3}$ cm^2/sec (Davies, 1966), and thickness of concentration boundary layer as δ = 0.085 cm (Van de Vate, 1972). The input data to the transport matrix [B] for each ventilation rate are listed in Appendix D. Matrix [B] is a square matrix having positive diagonal elements and negative off-diagonal elements, and the inverse of transport matrix, $[B]^{-1}$ exists. According to Liao and Feddes (1990), the matrix $[B]^{-1}$ is an irreducible, non-negative, square matrix. This implies that it is impossible to reduce matrix $[B]^{-1}$ to a block diagonal or block triangular form. From the theory of matrices, the eigenvalues of $[B]^{-1}$ are equal to the reciprocals of the eigenvalues of [B]. The transport matrix, [B], governs the time evolution of dust concentra-

tion histories when a step input is used to excite the system (Liao and Feddes, 1990).

2. Check the stability of the system:

After constructing the transport matrix [B] for each ventilation rate, the stability of the linear dynamic equation must be checked by calculating the eigenvalues corresponding to each transport matrix (Liao and Feddes, 1990) to make sure the system is stable. The general solution of the linear dynamic equation is:

$$\{n(t)\} = \sum_{k=1}^{L} C_k exp(-1/\lambda_k t)\{x^{(k)}\} + [D]\{G(s,s)\} \qquad (11)$$

where:

C_K = constants, dependent on the initial conditions,

λ_k = eigenvalues of $[B]^{-1}$, min, and

$\{x^{(k)}\}$ = eigenvectors of $[B]^{-1}$ corresponding to λ_k.

According to the stability criterion of the linear dynamic equation, all the eigenvalues for each transport matrix should be distinct and greater than zero. If some eigenvalues have a vanishing or negative real part, then the linear system is physically unstable and subject to uncontrolled growth with certain initial conditions or a bounded dust generation rate function. What affects the eigenvalues of transport matrix [B]? From equation (5), the transport

matrix [B] can be expressed as:

$$[B] = [H']^{-1} + [V]^{-1}[S'] + [V]^{-1}[Q]$$

It is obvious that once the lump dimensions have been decided, [H'], [V], [S'] will have definite values so that the only factor which affects the eigenvalues of matrix $[B]^{-1}$ is the ventilation airflow rate [Q]. An attempt was made to change the ventilation rate Q to see how it might influence the eigenvalues of matrix [B]. The results indicated that changing ventilation rate affects the magnitude of eigenvalues of [B], but not the sign of eigenvalues. Other parameters in equation (5) have a similar effect on the eigenvalues. When the lump number equals 12, there are always some negative eigenvalues. The negative eigenvalues disappear as the lump number decreases. When the transport matrix [B] had some negative eigenvalues, the linear dynamic equation did appear stable.

De Carlo (1989) explained that two kinds of stabilities exist via the usual time-invariant state model: 1. Bounded Input and Bounded State stability (BIBS), 2. Bounded Input and Bounded Output stability (BIBO). According to De Carlo's theory, the system is BIBS unstable if the state matrix ([B] matrix in the lumped-parameter model) has negative eigenvalues. However, it does not mean that BIBO is unstable. BIBO stability of the system depends on the observ-

ability of all unstable modes of the eigenvalues. In this model verification, the transport matrix [B] has negative eigenvalues thus being BIBS unstable; however, it is BIBO stable. Evidently, the negative eigenvalues can not be used to justify the stability of the linear dynamic equation. A more rigorous stability criterion is required.

RESULTS

Model Predictions and Experimental Results

Size distribution of the swine dust:

Although this experiment did not focus on swine dust particle size distribution, the dust concentration data did include these. The results of the particle size analysis show that the swine dust used in this project has an average particle aerodynamic diameter of 2 μm, 95 percent of the dust particle sizes are within the respirable range (< 5 μm) while approximately 45 percent of the particles are 2 μm in diameter (Figure 9).

Comparison of the measured with the predicted dust concentration

The simulated and measured equilibrium airborne dust concentrations of the 12 lumps at different ventilation rates with the three dust generation rates are listed in Tables 3, 4 and 5. All the measured values in Tables 3, 4 and 5 are the average of three measurements (replicates).

As shown in Tables 3, 4 and 5, the simulated results of equilibrium airborne dust concentration are quite uniform

and the concentrations are not significantly different among the 12 lumps at different ventilation rates. The difference between the highest and the lowest concentration values are in the range of 2.0 particles/cm^3 to 10 particles/cm^3 and similar for each dust generation rate.

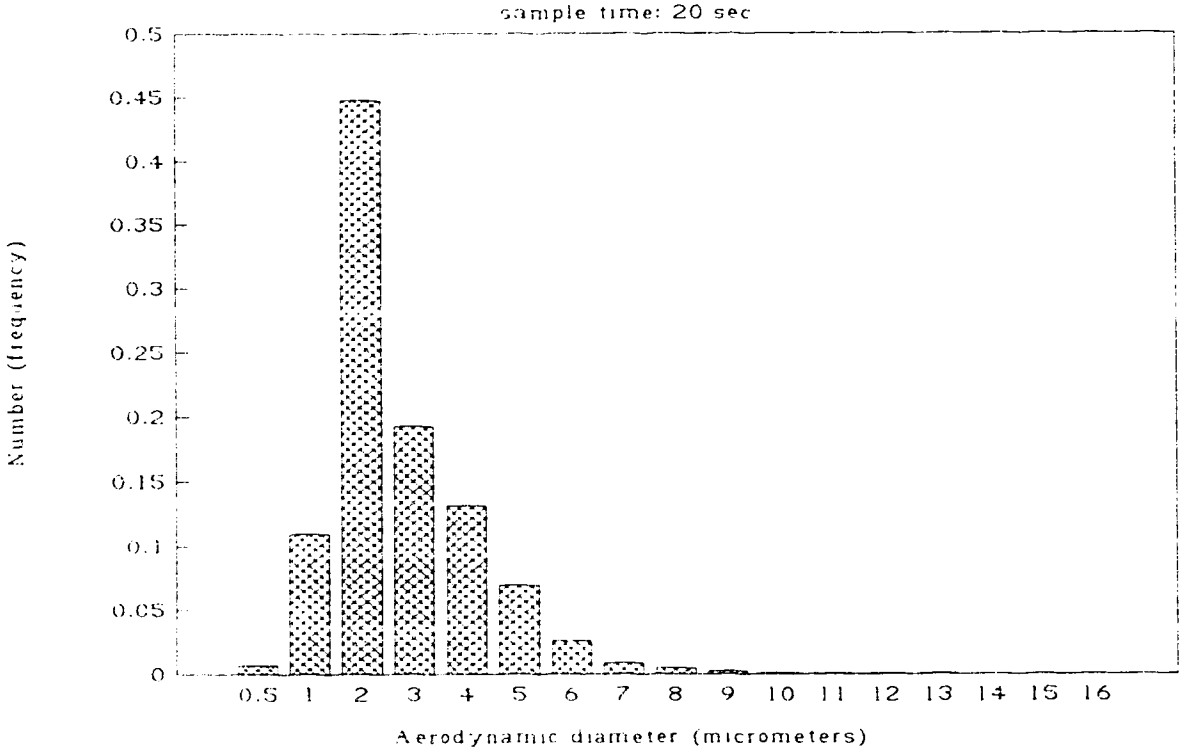

FIGURE 9. The size distribution of the test swine dust

Table 3. Equilibrium airborne dust concentration with a low dust generation rate (533×10^6 particles/min)

ventilation rate (m^3/hr)	lump number	dust concentration (particles/cm^3) predicted		measured	
300	1	63.6		65.1	
	2	67.4		64.0	
	3	68.6		67.9	
	4	64.1		98.5	
	5	68.2		62.2	
	6	69.2		44.4	
	7	69.3		198	
	8	70.5		156	
	9	70.4		116	
	10	71.1		245	
	11	73.0		143	
	12	71.9	Δ9.4	138	Δ201
900	1	27.5		144	
	2	29.2		56.7	
	3	29.8		51.1	
	4	27.7		87.6	
	5	29.4		80.3	
	6	30.0		50.2	
	7	29.8		219	
	8	30.3		150	
	9	30.4		67.0	
	10	30.4		139	
	11	31.1		93.5	
	12	30.9	Δ3.6	92.5	Δ169
1500	1	17.5		46.8	
	2	18.6		33.4	
	3	19.0		35.2	
	4	17.6		57.7	
	5	18.7		47.3	
	6	19.1		34.9	
	7	19.0		52.9	
	8	19.3		45.1	
	9	19.4		27.6	
	10	19.3		53.0	
	11	19.8		53.7	
	12	19.7	Δ2.3	33.1	Δ30.1

Δ=maximum - minimum

Table 4. Equilibrium airborne dust concentration with a medium dust generation rate (553×10^6 particles/min)

ventilation rate (m^3/hr)	lump number	dust concentration ($particles/cm^3$) predicted		measured	
300	1	65.3		94.0	
	2	69.7		49.0	
	3	71.3		55.3	
	4	65.9		152	
	5	70.1		87.3	
	6	71.8		62.0	
	7	71.0		286	
	8	73.1		167	
	9	73.7		81.7	
	10	72.8		321	
	11	74.4		267	
	12	75.2	Δ9.9	160	Δ272
900	1	28.3		114	
	2	30.1		58.8	
	3	30.9		49.3	
	4	28.5		96.8	
	5	30.3		83.9	
	6	31.1		55.9	
	7	30.5		175	
	8	31.4		141	
	9	31.8		68.1	
	10	31.2		162	
	11	31.8		121	
	12	32.2	Δ3.9	111	Δ126
1500	1	18.0		48.9	
	2	19.2		38.6	
	3	19.7		37.0	
	4	18.1		54.8	
	5	19.3		45.1	
	6	19.8		38.5	
	7	19.5		62.0	
	8	20.0		44.4	
	9	20.2		26.1	
	10	19.8		60.0	
	11	20.3		55.5	
	12	20.5	Δ2.5	39.3	Δ35.9

Δ=maximum - minimum

Table 5. Equilibrium airborne dust concentration with a high dust generation rate (665×10^6 particles/min)

ventilation rate (m^3/hr)	lump number	dust concentration (particles/cm^3) predicted		measured	
300	1	79.9		122	
	2	84.4		75.0	
	3	85.9		76.3	
	4	80.0		97.0	
	5	84.6		46.0	
	6	86.1		44.7	
	7	87.4		386	
	8	84.6		306	
	9	88.6		255	
	10	88.7		343	
	11	89.2		345	
	12	89.3	Δ9.4	251	Δ342
900	1	34.4		154	
	2	36.5		73.3	
	3	37.2		82.0	
	4	34.5		164	
	5	36.5		105	
	6	37.3		62.4	
	7	37.5		306	
	8	38.1		249	
	9	38.2		132	
	10	37.9		259	
	11	38.2		219	
	12	38.5	Δ4.1	129	Δ243
1500	1	21.9		84.9	
	2	23.3		70.3	
	3	23.8		55.0	
	4	22.0		83.0	
	5	23.3		74.1	
	6	23.8		55.9	
	7	23.9		94.5	
	8	24.2		55.5	
	9	24.4		37.6	
	10	24.1		86.6	
	11	24.4		79.6	
	12	24.5	Δ2.6	66.3	Δ56.9

Δ=maximum - minimum

The measured values in Tables 3, 4 and 5 indicate that the actual dust concentration in the test chamber was not as uniform as the simulated one. There were very large discrepancies between the measured and the predicted values especially in lumps 7, 8, 9, 10, 11 and 12 at the lower ventilation rate. Lumps near the inlet (lumps 1, 4, 7 and 10) had a greater discrepancy between the calculated and the measured values than the other lumps. The difference between the highest and the lowest concentration values range from 30 particles/cm^3 to 342 particles/cm^3. This large variation will be explored more in the comparison of the transient behavior of the airborne dust between treatments.

From the view point of height-from-floor level, the 12 lumps can be divided into upper and lower level. The upper level consists of lumps 1, 2, 3, 4, 5, and 6, with the others (7 - 12) in the lower level (Figure 7). With the predicted results, there is no obvious difference between the average dust concentrations at the upper level and those at the lower level lumps. This result is compared with the measured values in Tables 6, 7 and 8.

Table 6. Comparison of the average dust concentration of the upper level lumps with that of the lower level ones at the lower dust generation rate.

Average equilibrium dust concentration (particles/cm^3)						
Ventilation rate (m^3/hr)	upper level cal.	upper level meas.*	lower level cal.	lower level meas.*	difference cal.	difference meas.*
300	66.9	62.7	71.0	166	4.1	103
900	28.9	78.3	30.5	127	1.6	48.5
1500	18.4	42.8	19.4	44.4	1.0	1.6

Table 7. Comparison of the average dust concentration of the upper level lumps with that of the lower level lumps at the medium dust generation rate.

Average equilibrium dust concentration (particles/cm^3)						
Ventilation rate (m^3/hr)	upper level cal.	upper level meas.*	lower level cal.	lower level meas.*	difference cal.	difference meas.*
300	69.0	83.3	73.4	214	4.4	131
900	29.9	77.5	31.5	132	1.6	54.5
1500	19.0	46.3	20.0	45.4	1.0	0.9

Table 8. Comparison of the average dust concentration of the upper level lumps with that of the lower level lumps at a high dust generation rate

Average equilibrium dust concentration (particles/cm^3)						
Ventilation rate (m^3/hr)	upper level cal.	upper level meas.*	lower level cal.	lower level meas.*	difference cal.	difference meas.*
300	83.5	76.8	88.7	314	5.2	237
900	36.1	107	38.1	215	2.0	109
1500	23.0	70.5	24.3	70.0	1.3	0.5

* The measured values were the average of the three replicated runs.

Tables 6, 7 and 8 indicate that the average dust concentration difference between levels varies with ventilation rate. At high ventilation rates, the mean dust concentration difference between the two levels is very similar between the predicted and measured values, while a great discrepancy is observed at the low and medium ventilation rates. This discrepancy increases as dust generation rate increases.

The measured and predicted mean equilibrium airborne dust concentrations of the 12 sampling points (lumps) at different ventilation rates and dust generation rates are shown in Figures 10 to illustrate the trends. Minimum differences between the measured values and those predicted by the model occur at the high ventilation rate. The greatest deviation from the predictions occurs at medium ventilation rate. All the measured particle concentrations are higher than those calculated. The total airborne dust concentration decreases as the ventilation rate increases.

Table 9 also illustrates that, as the ventilation rate increases, the measured and the predicted airborne dust concentrations decrease. According to the model calculation, airborne dust concentrations should decrease by 57% when the ventilation rate is increased 3 times (300 m^3/hr to 900 m^3/hr). However, the actual airborne dust concentration

only decreased by 20% (average) for the three dust generation rates. When ventilation rate approaches 900 m^3/hr, the measured dust concentration attenuation (56%) was higher than that predicted by the model (36%).

Table 9. The measured and calculated airborne dust concentration decrease vs ventilation airflow rate increase

ventilation rate increase (m^3/hr)		airborne dust concentration decrease in the environmental chamber (%)					
		g1*		g2*		g3*	
from	to	meas.	cal.	meas.	cal.	meas.	cal.
300	900	11.9	56.9	30.6	56.9	17.6	56.9
300	1500	62.8	72.4	69.1	72.6	64.0	72.6
900	1500	57.7	36.4	55.5	36.4	56.4	36.4

* dust generation rate: g1 = low g2 = medium g3 = high

Transient airborne dust behavior:

Figures 11 to 13 show the comparison of the model-predicted transient responses of the airborne dust concentration at lump 5 with those measured for the different ventilation and dust generation rates. These graphs indicate that the fluctuations in the measured airborne dust concentration in lump 5 are much higher than those predicted by the model. At the low ventilation rate, the measured concentrations are lower than that simulated. However, they are higher than those predicted at the higher two ventila-

tion rates used. Also, these figures clearly indicate the departures in behavior of the local dust transport mechanisms that were assumed to be similar in all lumps.

Results of Analysis of Variance

The analysis of variance for the dust concentration is presented in Table 10. The F values in Table 10 indicate that the overall differences due to ventilation rate are significant, and dust generation rates also result in significant differences in airborne dust particle concentrations. The interaction between ventilation rate and dust generation rate is not significant. Figure 14 demonstrates the effects of the ventilation and dust generation rates on airborne dust concentration.

Table 10. Analysis of Variance

Source of Variance	Degrees of Freedom	Mean Squares	F value	Pr > F
V (ventilation)	2	284667.53	25.67	0.0001
D (dust generation)	2	90014.67	8.12	0.0031
V*D	4	7778.00	0.70	0.6010
Error 1 (Replicate(V*D))	18	11087.99		
L (level)	1	465829.00	52.25	0.0001
Error 2 (L*R(V*D))	18	8941.66		

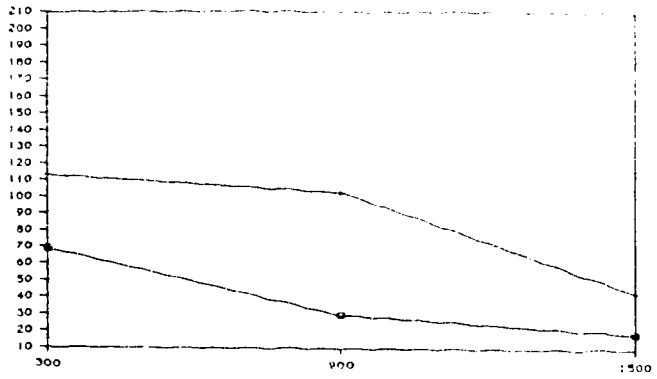

a) low dust generation rate

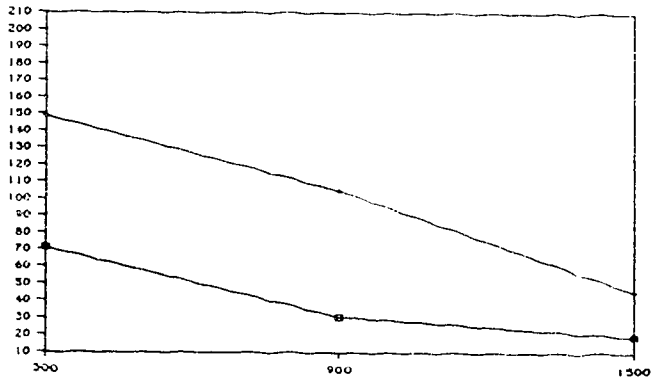

b) medium dust generation rate

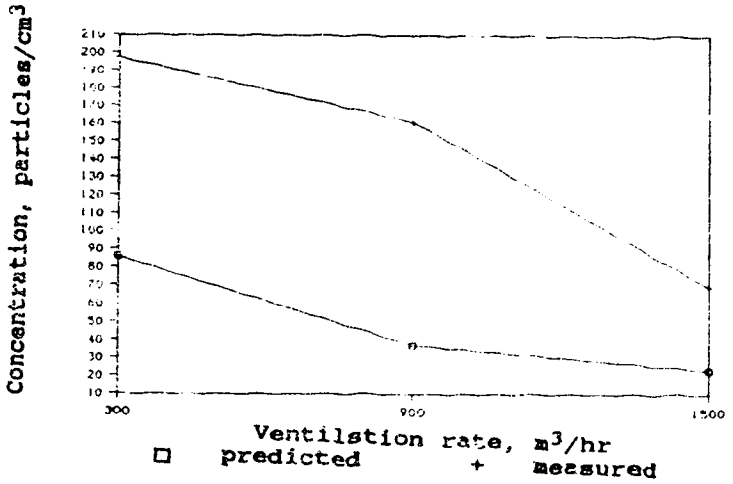

c) high dust generation rate

FIGURE 10. Comparison of average equilibrium dust particle concentration measurements and those predicted for different ventilation rates.

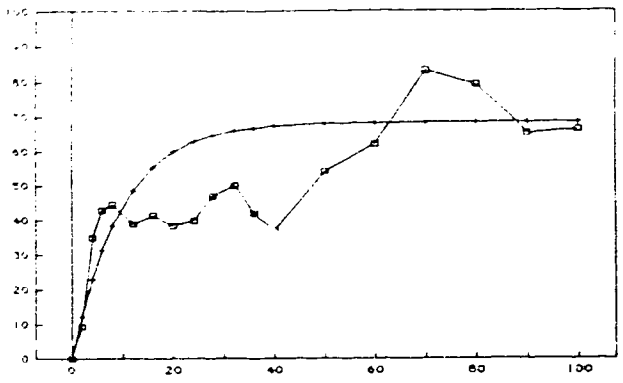

a) low dust generation rate

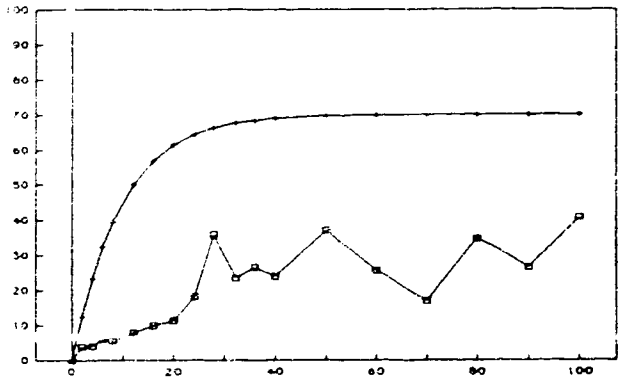

b) medium dust generation rate

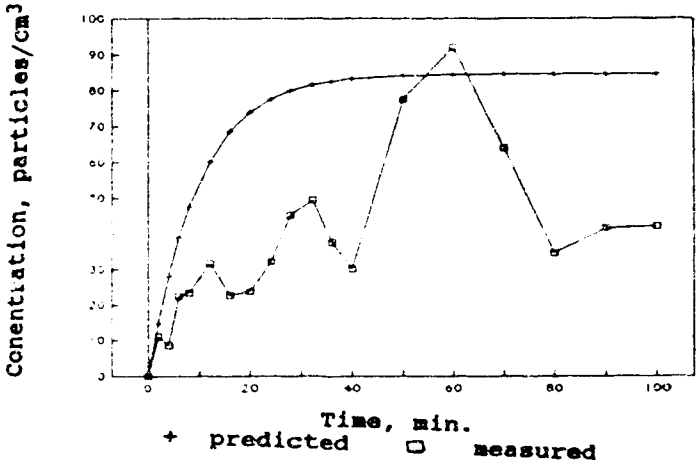

c) high dust generation rate

FIGURE 11. The transient behavior of the predicted airborne dust concentration and that measured in lump 5 at Q=300 m^3/hr.

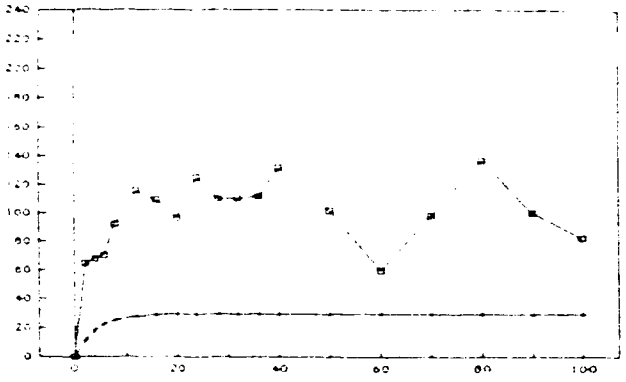

a) low dust generation rate

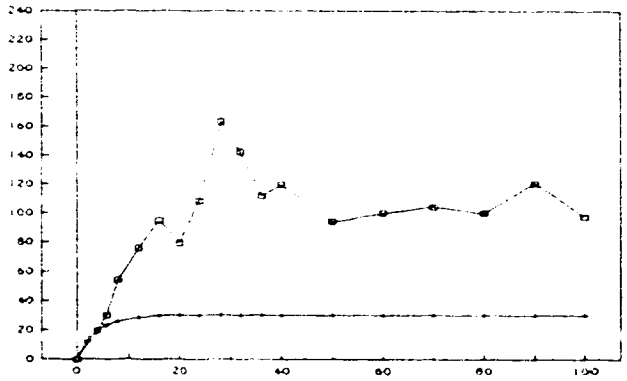

b) medium dust generation rate

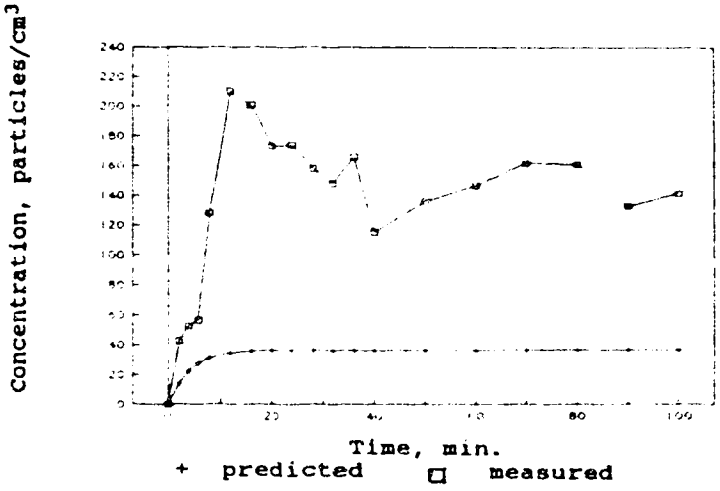

c) high dust generation rate

FIGURE 12. The transient behavior of the predicted airborne dust concentration and that measured in lump 5 at Q=900 m^3/hr.

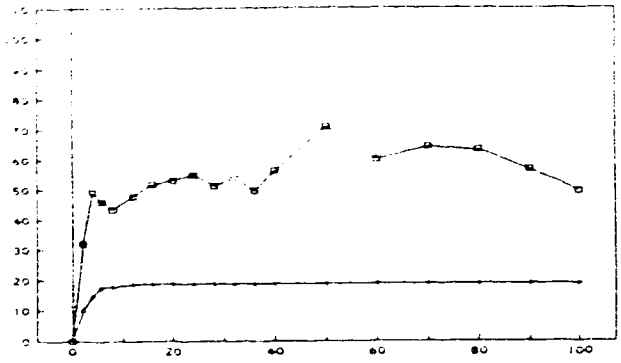

a) low dust generation rate

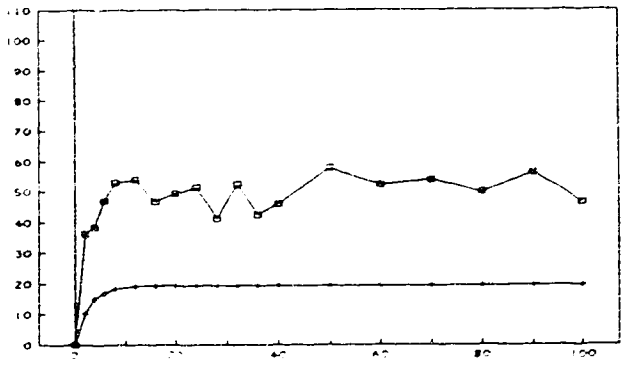

b) medium dust generation rate

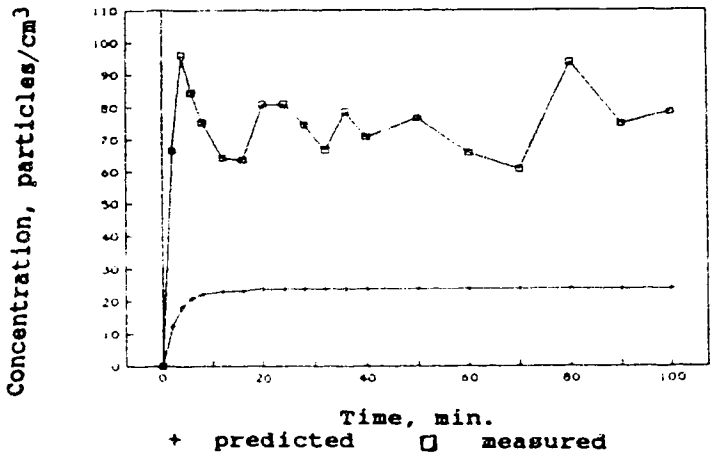

c) high dust generation rate

FIGURE 13. The transient behavior of the predicted airborne dust concentration and that measured in lump 5 at Q=1500 m^3/hr.

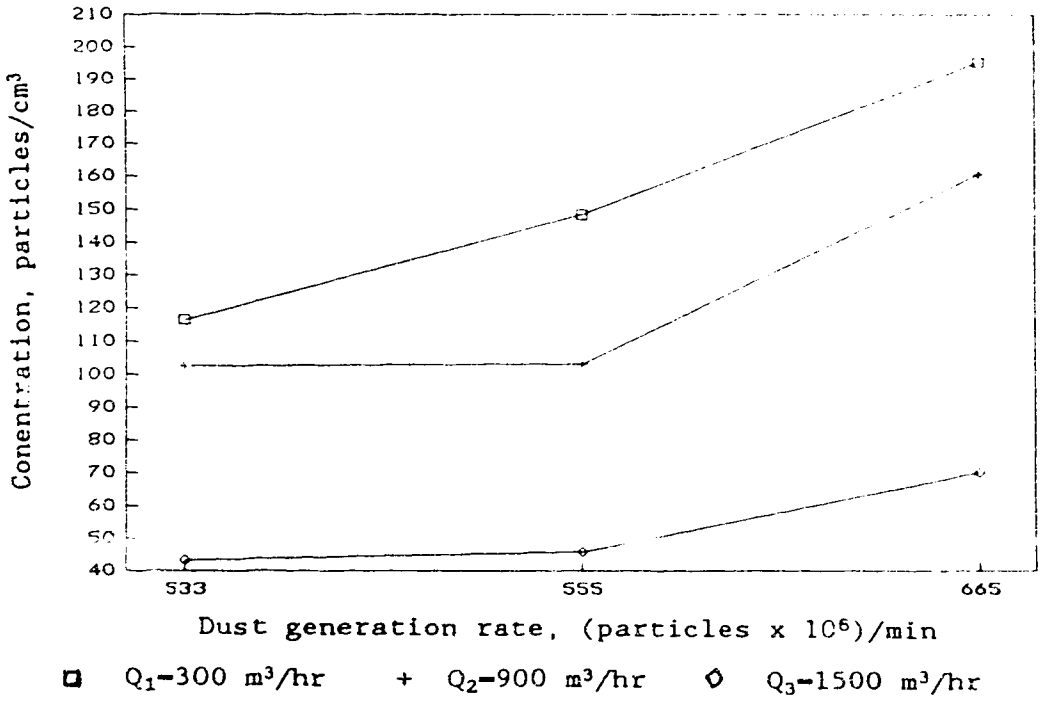

FIGURE 14. The effects of ventilation rate and dust generation rate on equilibrium airborne dust concentration.

DISCUSSION

From the dust concentration data, the most significant sources for the discrepancies occurring between the experimental and the predicted results may include the following:

1. The dust particle size uniformity: As mentioned previously, the dust particle size is the main factor affecting the dynamic behavior of the dust. The predicted values would agree with those measured if all the dust particles had a similar aerodynamic diameter of 2 μm (i.e., monodisperse). However, the dust particles have different sizes (polydisperse) (Figure 9). Their sizes range from 0.5 μm to larger than 15 μm. Figures 15 and 16 (Liao and Feddes, 1990(b)) indicate that when talcum powder was used as a test dust, good agreement occurred between the measured values and those calculated since talcum particles are much more uniform than the swine test dust particles. The lumped-parameter model is capble of predicting the ventilation rate required to maintain acceptable levels of airborne dust in confinement animal buildings based on dust generation rate. The accuracy of the model is influenced by the test dust particle size uniformity.

It is interesting to note that, if only those particles

with their size equal to 2 μm were counted as measured airborne dust concentration in the experimental chamber, the differences between the measured and those predicted by the model decreased dramatically (Figure 17).

2. Dust and dust generating system: Although the dust was agitated, the dust may not have been entirely homogeneous. Also the pitches of the augers were not exactly the same for each generation rate trial so the amount of the dust transported each time may not have been the same.

3. Instrument: According to Baron (1986) calibration of the APS can result in an error of 8-20%. Therefore, this error was applied randomly to the dust particle concentrations measured. Marshall and Mitchell (1990); Cheng et al. (1990) and Marshall et al. (1991) reported that because of the particle shape effect, the APS can underestimate non-spherical particles by an average of 25%. On the other hand, if particle sizes exceed that of the APS inner nozzle (the nozzle diameter is about 0.8 mm), particles may block the nozzle and affect the readings. APS has high resolution for particles in the range of 0.8-20 μm. Also errors may result in measuring the airflow rates.

Considering the APS measurement error, when the dust generation rates in the model calculation were doubled, the predicted particle concentrations agreed more closely with

with their size equal to 2 μm were counted as measured airborne dust concentration in the experimental chamber, the differences between the measured and those predicted by the model decreased dramatically (Figure 17).

2. Dust and dust generating system: Although the dust was agitated, the dust may not have been entirely homogeneous. Also the pitches of the augers were not exactly the same for each generation rate trial so the amount of the dust transported each time may not have been the same.

3. Instrument: According to Baron (1986) calibration of the APS can result in an error of 8-20%. Therefore, this error was applied randomly to the dust particle concentrations measured. Marshall and Mitchell (1990); Cheng et al. (1990) and Marshall et al. (1991) reported that because of the particle shape effect, the APS can underestimate nonspherical particles by an average of 25%. On the other hand, if particle sizes exceed that of the APS inner nozzle (the nozzle diameter is about 0.8 mm), particles may block the nozzle and affect the readings. APS has high resolution for particles in the range of 0.8-20 μm. Also errors may result in measuring the airflow rates.

Considering the APS measurement error, when the dust generation rates in the model calculation were doubled, the predicted particle concentrations agreed more closely with

5. The airflow matrix [Q]: Because the inherent limitations in the ability to predict airflow patterns in a ventilated airspace, the assumptions of the behavior of the local transport mechanisms made in each lump may depart from the actual situation and cause the system equation to underestimate dust concentrations; especially the dust concentrations of the lower level lumps at low and medium ventilation rates. A similar situation occurred when talcum powder was used as a test dust.

6. At the low ventilation rate, perhaps due to the larger dust particle size and the difference in the swine dust particle composition from that of talcum particles, swine dust particles can not reach the upper airspace thus the dust concentrations of the lower level lumps are evidently higher than those predicted. On the other hand, instability of the airflow patterns within a building may occur at low ventilation rates (Randall, 1980) and this is likely another reason leading to the greater discrepancy between the predicted and the measured values and the dust concentration fluctuation at low ventilation rates.

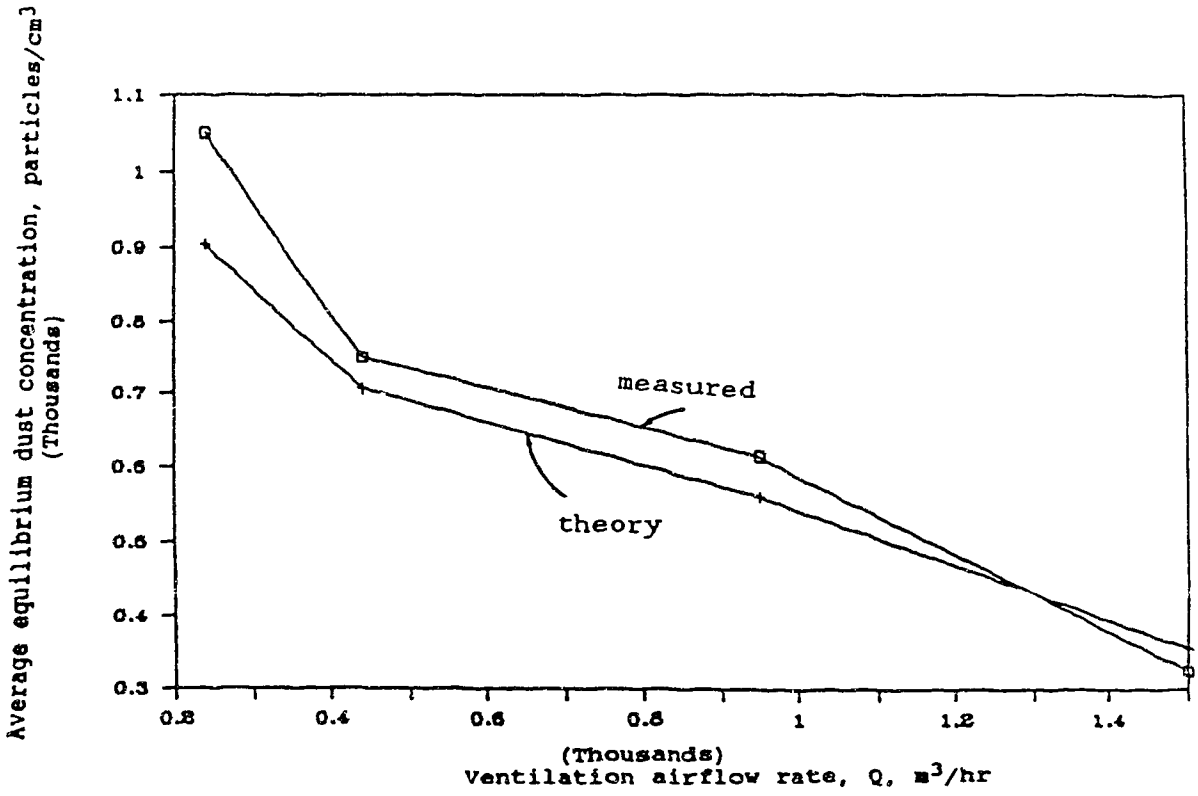

FIGURE 15. Comparison of average talcum particle concentration measurements and predicted results for different ventilation rate levels (Liao and Feddes, 1990(b)).

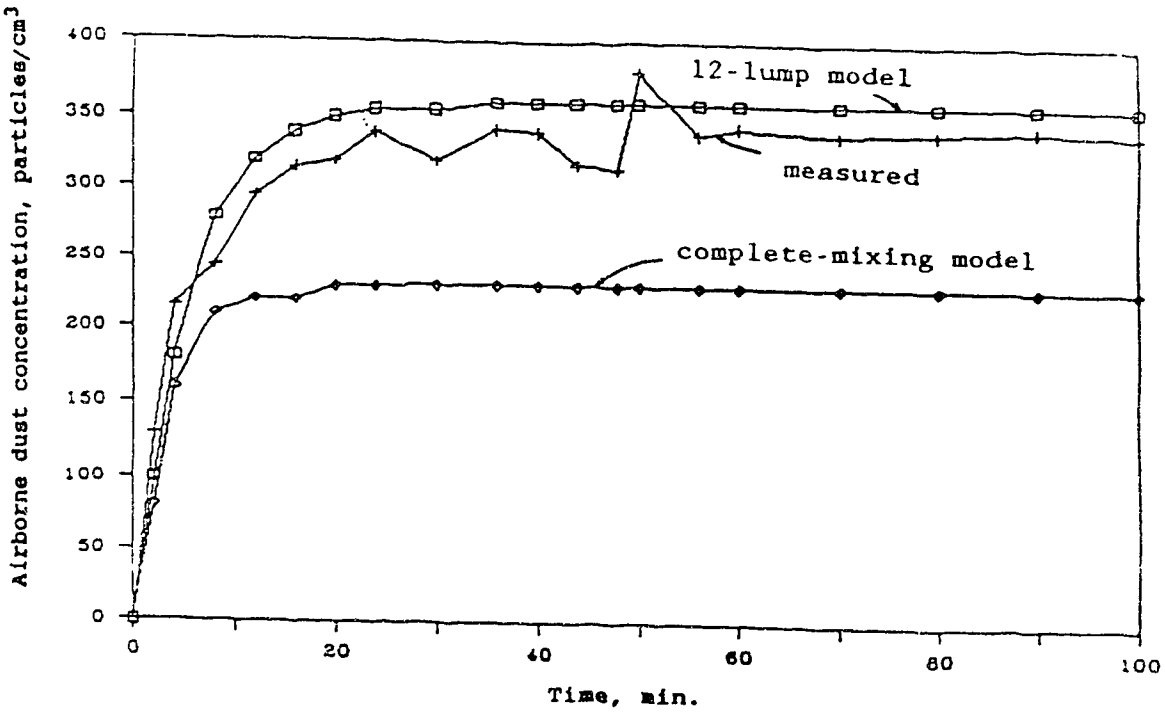

FIGURE 16. Comparison of transient behavior of predicted airborne talcum particle concentration from complete-mixing model and 12-lump model with that measured results in lump 5 at Q=443 m^3/hr (Liao and Feddes, 1990(b)).

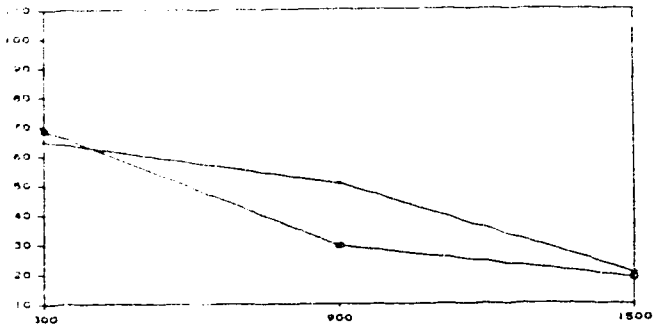

a) low dust generation rate

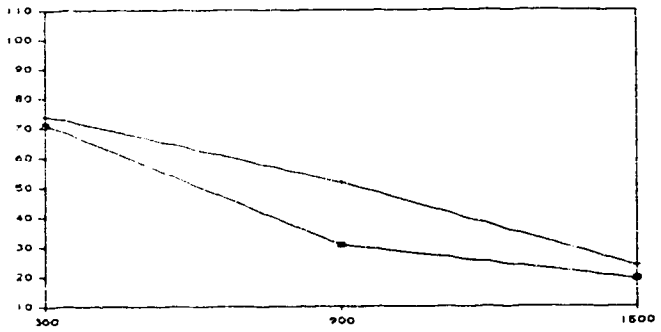

b) medium dust generation rate

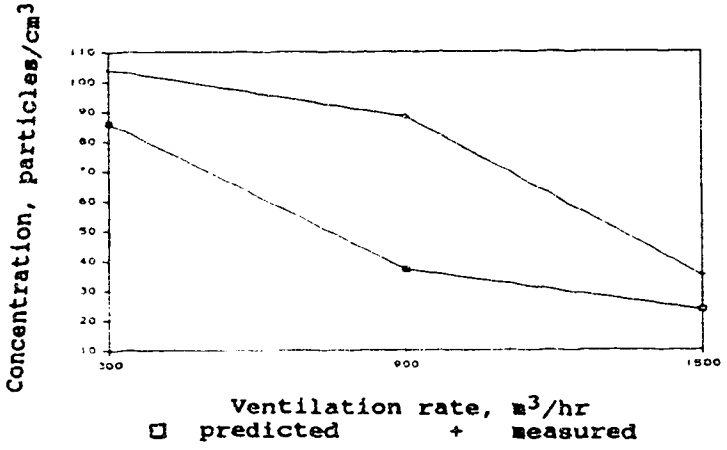

c) high dust generation rate

FIGURE 17. Comparison of the predicted average equilibrium dust concentration with those measured with a diameter of 2 (-0.02, +0.83) μm.

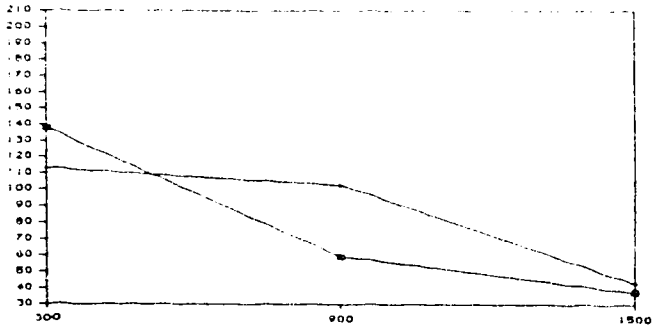

a) low dust generation rate

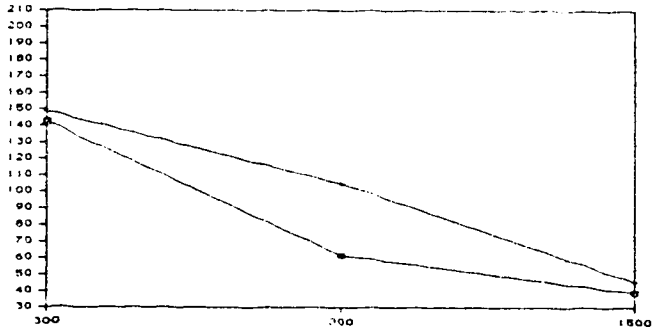

b) medium dust generation rate

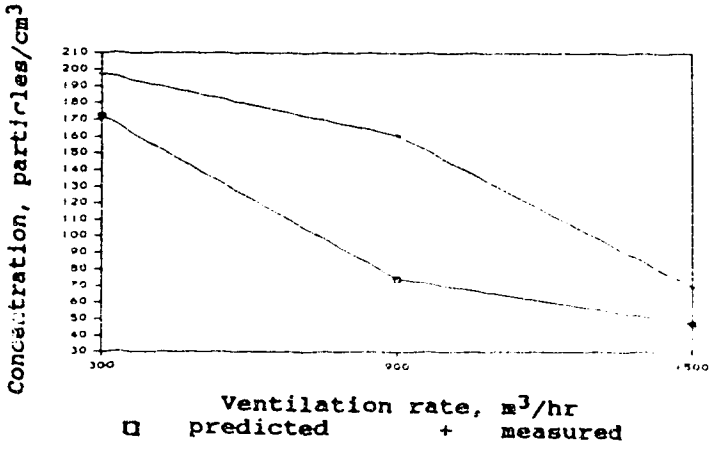

c) high dust generation rate

FIGURE 18. Comparison of the average equilibrium dust concentration measurements with those predicted when the dust generation rate is doubled.

SUMMARY AND CONCLUSIONS

The purpose of this thesis was to verify the lumped-parameter model for predicting airborne dust concentrations in a ventilated airspace using a swine test dust and to test the hypothesis that dust generation and ventilation rates do not affect airborne dust concentration. Conclusions drawn from this study are as follows:

1. Significant differences occurred between airborne dust concentrations for the ventilation and dust generation rates used. The interaction of ventilation rate and dust generation rate on dust concentration was not significant.

2. Levels of airborne dust change with height from the floor levels, and are affected by ventilation rate. The actual airborne dust concentration differences between the upper level lumps and the lower level ones are significantly different from those predicted by the model at low and medium ventilation rates.

3. When ventilation rate was increased from 300 m^3/hr to 900 m^3/hr, the measured airborne dust concentration dilution rate (20%) was lower than that predicted (57%). The measured dust concentration decreased by 56% when ventilation rate increased from 900 m^3/hr to 1500 m^3/hr;

however, the predicted dust concentration decrease was 36%.

4. The discrepancy between the calculated and measured results decreased when the measured dust concentration only consisted of particles having the size of 2 μm. The discrepancy ranged from a minimum of 3.9% to a maximum of 58%.

5. Swine dust used in this experiment study has an average aerodynamic diameter of 2 μm, 95% dust particles are less than 5 μm in size while approximately 45% of the particles are 2 μm in diameter.

6. The lumped-parameter model is capable of predicting the rate of ventilation required to maintain acceptable levels of airborne dust in confinement animal buildings based on dust generation rate.

7. The model calculation is a solution of a three dimensional lumped form of a control volume which represents the conservation of airflow mass. The model verification shows that the accuracy of the model is influenced by the test dust particle size uniformity. When swine dust was used as test dust, the discrepancy between the predictions made by the model and the measured results was greater than that using talcum particles.

8. Negative eigenvalues of transport matrix, [B], do not represent instability in the system equation; therefore, a more rigorous criterion to check the stability of the sys-

tem equation is required.

SUGGESTIONS FOR FUTURE STUDY

Advanced airborne dust control system design in ventilated animal housing is based on sophisticated mathematical models describing the dynamic behavior of airborne dusts. The lumped-parameter model is a deterministic model, i.e., each variable and parameter in the model can be assigned a definite fixed number, or a series of fixed numbers, for any given set of conditions. In the model derivation, spatial dust concentration variation in each lump is ignored and mixing is considered to be homogeneous throughout the lump. The suggestions for future study , therfore, are: 1. Carry out a stochastic analysis of the dynamic behavior of airborne dust in ventilated animal housing, and 2. Determine the uncertainties in the airflow calculation from the measured data by an error analysis technique.

BIBLIOGRAPHY

ASHRAE Handbook of Fundamentals. 1989. American Society of Heating, Refrigerating, and Air Conditioning Engineers, New York, NY.

Barber, E. M., and J. R. Ogilvie. 1982. Incomplete mixing in ventilated airspace. Part I. Theoretical considerations. Canadian Agri. Eng. 24(1): 25 - 29.

Baron, P. A. 1986. Calibration and use of the aerodynamic particle sizer (APS 3300). Aerosol Science and Tech., 5: 55 - 67

Boon, C. R. 1978. Airflow Patterns and temperature distribution in an experimental piggery. J. Agri. Eng. Research, 23: 129 - 139.

Brannigan, P. G., and J. B. McQuitty. 1971. The influence of ventilation on distribution and dispersal of atmospheric gaseous contaminants. Canadian Agri. Eng. 13(2): 69 - 75.

Bundy, D. S. and T. E. Hazen. 1975. Dust levels in swine confinement systems associated with different feeding methods. Trans. of the ASAE, 18(2): 137 - 139 & 144.

Bundy, D. S. 1984. Rate of dust decay as affected by relative humidity, ionization and air movement. Trans. of the ASAE, 27(3): 865 - 870.

Burnett, W. E. 1969. Odor transport by particulate matter in high density poultry houses. Poultry Science 48: 182 - 184

Carpenter, G. A. 1986. Dust in livestock buildings-review of some aspects. J. of Agri. Eng. Research 33: 227 - 241.

Cheng, Y. S., B. T. Chen and H. C. Yeh. 1990. Behavior of isometric non-spherical aerosol particles in the aerodynamic particle sizer. J. Aerosol Sci. Vol 21(5): 701 - 710.

Chiba, L. I., E. R. Peo, A. J. Leewis, M. C. Brumm, R. D. Fritschen, and J. D. Crenshaw. 1985. Effect of dietary fat on pig performance and dust levels on modified-open-front and environmentally regulated confinement buildings. J. of Animal Sci., 61(4): 763 - 780.

Choi, H. L., L. D. Albright, M. B. Timmons, and Z. Warhaft. 1988. An application of the K-Epsilon turbulence model to predict air distribution in a slot-ventilated enclosure. Trans. of the ASAE, 31(6): 1804 - 1814.

Choi, H. L., L. D. Albright, and Z. Warhaft. 1987. Air velocity and contaminant distribution in a slot -ventilated enclosure. Paper No 87-4036. ASAE, St. Joseph, MI.

Curtis, S. E., J. G. Drummond, K. W. Kelley, D. G. Grunloh, V. J. Meares, H. W. Norton, and A. H. Jensen. 1975. Diurnal and annual fluctuations of aerial bacterial and dust levels in enclosed swine houses. J. of Animal Sci., 41(5): 150[illegible] - 1511.

Davies, C. N. 1966. Deposition from moving aerosols. In Aerosol Science. Davies, C. N. (ed.) pp. 393 - 446. Academic Press, New York, NY.

De Corlo, R. A. 1989. Linear Systems. Prentice Hall Inc. Englewood Cliffs, NJ.

De Praetere, K., and Van Der Biest, W. 1989. Airflow patterns and their relation to ammonia distribution. In: V. A. Dodd and P. M. Grace Eds. Agri. Eng. Proc. 11th Int. Congress of CIGR, Vol. (2): 1457 - 1484. A. A. Balkema, Rotterdam.

Donham, K. J., W. Popendorf, U. Palmgren, and L. Larsson. 1986. Characterization of dusts collected from swine confinement buildings. American J. of Industrial Medicine 10: 294 - 297.

Dyment, J. 1976. Air filtration. In: Control of the Animal House Environment. T. M. McSheehy (ed.). Laboatory Animals, Ltd., London. pp. 209 -246.

Friedlander, S. K. 1977. Smoke, dust and haze. Fundamentals of aerosol behavior. John Wiley and Sons, New York, NY.

Gosman, A. D. and P. V. Nielsen, A. Restivo and J. H. Whitelaw. 1980. The flow properties of rooms with a small ventilation opening. Trans. ASME. J. Fluids Eng. 102: 316 - 323

Greenfield, M. A., R. L. Koontz, and D. F. Hausknecht. 1971. Comparison of experimental and theory for the coagulation of aerosols. J. of Colloid and Interface Sci., 35(1): 102 - 113.

Grub, W., C. A. Rollo, and J. R. Howes. 1965. Dust and air filtration in animal shelters. Trans. of the ASAE, 8(3): 338-339, 352.

Gustafsson, G. 1989. Mass balance of dust in houses of pigs. In: V. A. Dodd and P. M. Grace Eds. Agri. Eng. Proc. 11th Int. Congress of CIGR, Vol. (2): 1485 - 1470 A. A. Balkema, Rotterdam.

Harry, E. G. 1978. Air pollution in farm buildings and methods of control: A review. Avian Pathology 7: 411 - 454.

Heber, A. J., M. Stroik, J. M. Faubion, and L. H. Willard. 1988(a). Size distribution and identification of aerial dust particles in swine finishing buildings. Trans. of the ASAE, Vol. 31(3): 882 - 887.

Heber, A. J., M. Stroik, J. L. Nelssen, and D. A. Nichols. 1988(b). Influence of environmental factors on concentrations and inorganic content of aerial dust in swine finishing buildings. Trans. of the ASAE, Vol. 31(3): 875 - 881.

Himmelblau D. M., and K. B. Bischoff. 1968. Process analysis and simulation. Deterministic systems. John Wiley and Sons, New York, NY.

Hinds, W. C. 1982. Aerosol Technology. John Wiley and Sons. New York, NY.

Honey, L. F., and J. B. McQuitty. 1979. Some physical factors affecting dust concentrations in a pig facility. Canadian Agri. Eng. 21: 9 - 14.

Huang, C. M., M. Kerker, and E. Matijevic. 1970. The effect of Brownian coagulation gradient coagulation, turbulent coagulation, and wall losses upon the particle size distribution of an aerosol. J. of Colloid and Interface Sci. 33(4): 529 - 538.

Janni, K. A., P. T. Redig, J. Newman, and J. Mulhausen. 1984. Respirable aerosol concentrations in turkey grower buildings. Paper No. 84-4522, ASAE St. Joseph, MI.

Jorgrnson, R. 1983. Fan Engineering (8th edition). Buffals Forge Company. Buffalo, NY.

Koon, J., J. R. Howes, W. Grub, and C. A. Rollo. 1963. Poultry dust: origin and composition. Agri. Eng., 44 (11): 608 - 609.

Langstroth, G. O., and T. Gillespie. 1947. Coagulation and surface losses in disperse system in still and turbulent air. Canadian J. of Research 25(B): 455 -471.

Leonard, J. J. 1986. Design and control of ventilation inlets for animal housing. Unpublished Ph.D. Thesis. University of Alberta, Edmonton, AB.

Liao, C. M. 1989. The dynamics of gaseous pollutants. Unpublished Ph.D. Thesis. Iowa State University, Ames, Iowa.

Liao, C. M., and J. J. R. Feddes. 1989. Modelling and analysis of dynamic behavior of airborne dust in a ventilated airspace. Paper No. PNR89-402. ASAE St. Joseph, MI.

Liao, C. M., and J. J. R. Feddes. 1990(a). Mathematical analysis of a lumped-parameter model for describing the behavior of airborne dust in animal housing. Applied Mathematical Modelling. 14: 248 - 257.

Liao, C. M., and J. J. R. Feddes. 1990(b). A lumped-parameter
model for predicting airborne dust concentrations in a ventilated airspace. Paper No. 90 - 125. CSAE Saskatoon, SK.

Lindauer, G. C., and A. W. Castleman, Jr. 1971. Behavior of aerosols undergoing Brownian coagulation and gravitational settling in closed system. J. of Aerosol Sci., 2:85 - 91

Marshall, I. A. and J. P. Mitchell. 1990. Calibration of a TSI Aerodynamic Particle Sizer with monodisperse non-spherical particles. J. Aerosol Sci. Vol. 21, Suppl. 1: s613 - s616.

Marshall, I. A., J. P. Mitchell and W. D. Griffiths. 1991. The behavior of regular-shaped non-spherical particles in a TSI Aerodynamic Particle Sizer. J. Aerosol Sci. Vol. 22(1): 73 - 89.

McQuitty, J. B., J. J. R. Feddes, and J. J. Leonard. 1985. Airquality in commercial laying barns. Canadian Agri. Eng., 27(1): 13 - 19.

Meyer, D. J. and H. B. Manbeck. 1986. Dust levels in mechanically ventilated swine barns. Paper No. 86-4042, ASAE St. Joseph, MI.

Mercer, T. T. 1978. Respirable fraction of airborne dust: Quantitative descriptions, formal definations, and performance characteristics of samplers matched to them. J. of Testing and Evaluation 6(1): 9 -19.

Mueller, W. 1984. Hog houses and human health. National Hog Farmer 29(1): 84 - 89.

Nielsen, P. V. 1973. Calculation of air movement in a ventilated room. Ingeniorens Ugeblad. 5: 31 - 32.

Nielsen, P. V., A. Restivo, and J. H. Whitelaw. 1978. The velocity characteristics of ventilated rooms. Trans. of ASME. J. Fluids Engr., 100: 291 - 298.

Nilsson, C. 1982. Dust investigations in pig houses. Swedish University of Agricultural Science, Department of Farm Buildings, Division of Farm Building Constructions, Report 25.

Okuyama, K., Y. Kousaka, and T. Yoshida. 1976. Behavior of aerosols undergoing Brownian coagulation, Brownian diffussion and gravitational settling in a closed chamber. J. of Chem. Eng. of Japan, 9(2): 140 - 146.

Okuyama, K., and Y. Kousaka. 1977. Turbulent coagulation of aerosols in a stirred tank. J. Chem. Eng. of Japan, 10(2): 142 - 147.

Okuyama, K., Y. Kousaka, and M. Adachi. 1980. Coagulation and deposition of aerosol particles in a flow type chamber. J. Aerosol Sci., 11: 11 - 22.

Phillips, P. A. 1986. Dust levels in mechanically versus naturally ventilated hog barns. Paper No. 86-4041, ASAE St. Joseph, MI.

Randall, J. M. 1977. The prediction of airflow pattern in livestock buildings. J. Agri. Eng. Research, 20: 199 - 215.

Randall, J. M. 1980. Selection of piggery ventilation systems and penning layouts based on the cooling effects of air speed and temperature. J. Agri. Eng. Research, 25: 169 - 187.

Randall, J. M., and V. A. Battams. 1976. The observed influence of surface obstructions on the airflow pattern within livestock buildings. J. Agri. Eng. Research, 21: 33 - 39.

Randall, J. M., and V. A. Battams. 1979. Stability criteria for airflow patterns in livestock buildings. J. Agri. Eng. Research, 24: 361 - 374.

Randolph, A. D., and M. A. Larson. 1962. Transient and steady state size distribution in continuous mixed suspension crystallizers. Am. Inst. Chem. Eng. Journal, 8(5): 639 - 645

Robertson, J. F. 1989. Effect of purge ventilation on the concentration of airborne dust in pig buildings. In: V. A. Dodd and P. M. Grace Eds. Agri. Eng. Proc. 11th Int. Congress of CIGR, Vol. (2): 1495 - 1499. A. A. Balkema, Rotterdam.

SAS Institute Inc. 1989. SAS User's Guide: Statistics, Version 6.06. Cary, NC.

Timmons, M. B., L. D. Albright, R. E. Torrance, and R. B. Furry. 1980. Experimental and numerical study of air movement in slot-ventilated enclosures. Trans. ASHRAE 86(1):221 - 239.

Van de Vate, J. F. 1972. The thickness of the stagnant air layer in aerosol contaminants and the aerodynamic diameter of aggregates of small spheres. J. of Collide Int. Sci. 41(2): 194 - 197.

Van Wicklen, G. L., and B. W. Mitchell. 1986. The respirable aerosol concentration in a FAPP poultry house. Paper No. 86-4534. ASAE St. Joseph, MI.

Van Wicklen, G. L., and M. F. Yoder. 1988. Respirable aerosol concentration in an enclosed swine nursery. Trans. of the ASAE, 31(6): 1798 - 1803.

Randall, J. M. 1977. The prediction of airflow pattern in livestock buildings. J. Agri. Eng. Research, 20: 199 - 215.

Randall, J. M. 1980. Selection of piggery ventilation systems and penning layouts based on the cooling effects of air speed and temperature. J. Agri. Eng. Research, 25: 169 - 187.

Randall, J. M., and V. A. Battams. 1976. The observed influence of surface obstructions on the airflow pattern within livestock buildings. J. Agri. Eng. Research, 21: 33 - 39.

Randall, J. M., and V. A. Battams. 1979. Stability criteria for airflow patterns in livestock buildings. J. Agri. Eng. Research, 24: 361 - 374.

Randolph, A. D., and M. A. Larson. 1962. Transient and steady state size distribution in continuous mixed suspension crystallizers. Am. Inst. Chem. Eng. Journal, 8(5): 639 - 645

Robertson, J. F. 1989. Effect of purge ventilation on the concentration of airborne dust in pig buildings. In: V. A. Dodd and P. M. Grace Eds. Agri. Eng. Proc. 11th Int. Congress of CIGR, Vol. (2): 1495 - 1499. A. A. Balkema, Rotterdam.

SAS Institute Inc. 1989. SAS User's Guide: Statistics, Version 6.06. Cary, NC.

Timmons, M. B., L. D. Albright, R. E. Torrance, and R. B. Furry. 1980. Experimental and numerical study of air movement in slot-ventilated enclosures. Trans. ASHRAE 86(1):221 - 239.

Van de Vate, J. F. 1972. The thickness of the stagnant air layer in aerosol contaminants and the aerodynamic diameter of aggregates of small spheres. J. of Collide Int. Sci. 41(2): 194 - 197.

Van Wicklen, G. L., and B. W. Mitchell. 1986. The respirable aerosol concentration in a FAPP poultry house. Paper No. 86-4534. ASAE St. Joseph, MI.

Van Wicklen, G. L., and M. F. Yoder. 1988. Respirable aerosol concentration in an enclosed swine nursery. Trans. of the ASAE, 31(6): 1798 - 1803.

APPENDIES

Appendix A: Assumptions for the Population Model

Assumptions are as follows:

1. No gas-to-particle conversion occurs within the system.

2. No external forces act on the particle other than gravity.

3. Particles have an aerodynamic equivalent diameter and are electrically neutral.

4. Particles collide with each other to form a single new spherical particle whose mass is the same as the combined mass of the two smaller particles.

5. The dust particle concentration is spatially uniform in the system volume except across the boundary layer where the concentration changes linearly within the layer.

Appendix B: Assumptions for the Lumped-Parameter Model

The following assumptions are made:

1. Finite lump model. There are m lumps with $m \geq 1$.

2. Ventilation air transport system. A flow rate $Qij \geq 0$ gives the airflow from the j^{th} to the i^{th} lump for $i \neq j$ with $1 \leq i, j \leq m$. A flow rate Qis gives the input flow and a flow rate Qei gives the output flow for the i^{th} lump for $1 \leq i \leq m$.

3. Airflow transfer system. A transfer flow Qij assumed to be entirely generated by entrainment air into the jet stream from the supply air duct. Therefore, the transfer airflow rate occurs at interface of the lump can be expressed as $Qij=Fij(\beta)Q$, in which $Fij(\beta)$ is the function of entrainment ratio (β) and can be calculated by the entrainment theory for air jets (ASHRAE Handbook of Fundamentals, 1989), and Q is the total volumetric flow rate of outdoor air supplied to the whole system.

4. The dominant mechanisms of the dynamic behavior of dust in ventilated airspace are turbulent coagulation, turbulent diffusive deposition, gravitational sedimentation, and airflow rate.

5. Particles have an aerodynamic equivalent diameter and are electrically neutral.

6. The dust concentration is spatially uniform in each lump except within the concentration boundary layer, and the concentration changes linearly within this layer.

Appendix C: EMS Table

There are a total of 324 values of dust concentration data. In order to calculate the Expected Mean Square (EMS), the lump number was reduced from 12 to 4 since computer system does not have enough memory to calculate the General Linear Model (GLM). Therefore, statistical analysis was done in two steps: first, obtain the table of EMS, and secondly, carry out the analysis of variance (ANOVA) test.

General Linear Models Procedure

Source	Type III Expected Mean Square
VENRA	Var(Error) + 2 Var(REPL*LEVE(VENR*DGER)) + 4 Var(REPL(VENRA*DGERA)) + Q(VENRA,VENRA*DGERA,VENRA*LEVEL, VENRA*DGERA*LEVEL,VENRA*LUMP,VENRA*DGERA*LUMP,VENRA*LEVEL*LUMP,VENR*DGER*LEVEL*LUMP)
DGERA	Var(Error) + 2 Var(REPL*LEVE(VENR*DGER)) + 4 Var(REPL(VENRA*DGERA)) + Q(DGERA,VENRA*DGERA,DGERA*LEVEL, VENRA*DGERA*LEVEL,DGERA*LUMP,VENRA*DGERA*LUMP,DGERA*LEVEL*LUMP,VENR*DGER*LEVEL*LUMP)
VENRA*DGERA	Var(Error) + 2 Var(REPL*LEVE(VENR*DGER)) + 4 Var(REPL(VENRA*DGERA)) + Q(VENRA*DGERA,VENRA*DGERA*LEVEL,VENRA*DGERA*LUMP,VENR*DGER*LEVEL*LUMP)
REPL(VENRA*DGERA)	Var(Error) + 2 Var(REPL*LEVE(VENR*DGER)) + 4 Var(REPL(VENRA*DGERA))
LEVEL	Var(Error) + 2 Var(REPL*LEVE(VENR*DGER)) + Q(LEVEL,VENRA*LEVEL,DGERA*LEVEL,VENRA*DGERA*LEVEL,LEVEL*LUMP, VENRA*LEVEL*LUMP,DGERA*LEVEL*LUMP,VENR*DGER*LEVEL*LUMP)
VENRA*LEVEL	Var(Error) + 2 Var(REPL*LEVE(VENR*DGER)) + Q(VENRA*LEVEL,VENRA*DGERA*LEVEL,VENRA*LEVEL*LUMP,VENR*DGER*LEVEL*LUMP)
DGERA*LEVEL	Var(Error) + 2 Var(REPL*LEVE(VENR*DGER)) + Q(DGERA*LEVEL,VENRA*DGERA*LEVEL,DGERA*LEVEL*LUMP,VENR*DGER*LEVEL*LUMP)
VENRA*DGERA*LEVEL	Var(Error) + 2 Var(REPL*LEVE(VENR*DGER)) + Q(VENRA*DGERA*LEVEL,VENR*DGER*LEVEL*LUMP)
REPL*LEVE(VENR*DGER)	Var(Error) + 2 Var(REPL*LEVE(VENR*DGER))
LUMP	Var(Error) + Q(LUMP,VENRA*LUMP,DGERA*LUMP,VENRA*DGERA*LUMP,LEVEL*LUMP,VENRA*LEVEL*LUMP,DGERA*LEVEL*LUMP, VENR*DGER*LEVEL*LUMP)
VENRA*LUMP	Var(Error) + Q(VENRA*LUMP,VENRA*DGERA*LUMP,VENRA*LEVEL*LUMP,VENR*DGER*LEVEL*LUMP)
DGERA*LUMP	Var(Error) + Q(DGERA*LUMP,VENRA*DGERA*LUMP,DGERA*LEVEL*LUMP,VENR*DGER*LEVEL*LUMP)
VENRA*DGERA*LUMP	Var(Error) + Q(VENRA*DGERA*LUMP,VENR*DGER*LEVEL*LUMP)
LEVEL*LUMP	Var(Error) + Q(LEVEL*LUMP,VENRA*LEVEL*LUMP,DGERA*LEVEL*LUMP,VENR*DGER*LEVEL*LUMP)
VENRA*LEVEL*LUMP	Var(Error) + Q(VENRA*LEVEL*LUMP,VENR*DGER*LEVEL*LUMP)
DGERA*LEVEL*LUMP	Var(Error) + Q(DGERA*LEVEL*LUMP,VENR*DGER*LEVEL*LUMP)
VENR*DGER*LEVEL*LUMP	Var(Error) + Q(VENR*DGER*LEVEL*LUMP,

Appendix D: The Dat[illegible] the Transfer Matrix [B] for the Thre[illegible]ntilation Rates Used

$Q = 300\ m^3/nr$

$$[B] = \begin{pmatrix}
8.6561 & -2.7378 & 0 & -2.7378 & 0 & 0 & -2.7378 & 0 & 0 & 0 & 0 & 0 \\
3.1428 & 11.3776 & -2.7378 & 0 & -2.7378 & 0 & 0 & 2.7378 & 0 & 0 & 0 & 0 \\
0 & -3.1428 & 8.6561 & 0 & 0 & 2.7378 & 0 & 0 & 2.7378 & 0 & 0 & 0 \\
-2.7378 & 0 & 0 & 8.6561 & 2.7378 & 0 & 0 & 0 & 0 & 2.7378 & 0 & 0 \\
0 & 2.7378 & 0 & 3.1428 & 11.3776 & -2.7378 & 0 & 0 & 0 & 0 & 2.7378 & 0 \\
0 & 0 & -2.7378 & 0 & -3.1428 & 8.6561 & 0 & 0 & 0 & 0 & 0 & 2.7378 \\
-2.7378 & 0 & 0 & 0 & 0 & 0 & 8.2580 & 2.7378 & 0 & 2.7378 & 0 & 0 \\
0 & -2.7378 & 0 & 0 & 0 & 0 & 2.7378 & 10.9794 & 2.7378 & 0 & 2.7378 & 0 \\
0 & 0 & -2.7378 & 0 & 0 & 0 & 0 & 2.7378 & 8.4605 & 0 & 0 & 2.7378 \\
0 & 0 & 0 & -2.7378 & 0 & 0 & -2.7378 & 0 & 0 & 8.2580 & 2.7378 & 0 \\
0 & 0 & 0 & 0 & -2.7378 & 0 & 0 & 2.7378 & 0 & 2.7378 & 10.9794 & 2.7378 \\
0 & 0 & 0 & 0 & 0 & 2.9403 & 0 & 0 & 2.7378 & 0 & 2.7378 & 8.4605
\end{pmatrix} (min^{-1})$$

$Q = 900\ m^3/hr$

$$[B] = \begin{pmatrix}
25.8929 & -8.2134 & 0 & -8.2134 & 0 & 0 & -8.2134 & 0 & 0 & 0 & 0 & 0 \\
-9.4284 & 34.0900 & -8.2134 & 0 & 8.2134 & 0 & 0 & 8.2134 & 0 & 0 & 0 & 0 \\
0 & -9.4284 & 25.8929 & 0 & 0 & -8.2134 & 0 & 0 & 8.2134 & 0 & 0 & 0 \\
-8.2134 & 0 & 0 & 25.8929 & 8.2134 & 0 & 0 & 0 & 0 & 8.2134 & 0 & 0 \\
0 & 8.2134 & 0 & -9.4284 & 34.0900 & -8.2134 & 0 & 0 & 0 & 0 & 8.2134 & 0 \\
0 & 0 & -8.2134 & 0 & -9.4284 & 25.8929 & 0 & 0 & 0 & 0 & 0 & 8.2134 \\
-8.2134 & 0 & 0 & 0 & 0 & 0 & 24.6848 & -8.2134 & 0 & 8.2134 & 0 & 0 \\
0 & 8.2134 & 0 & 0 & 0 & 0 & 8.2134 & 32.8818 & 8.2134 & 0 & 8.2134 & 0 \\
0 & 0 & -8.2134 & 0 & 0 & 0 & 0 & 8.2134 & 25.2923 & 0 & 0 & 8.2134 \\
0 & 0 & 0 & -8.2134 & 0 & 0 & 8.2134 & 0 & 0 & 24.6848 & 8.2134 & 0 \\
0 & 0 & 0 & 0 & -8.2134 & 0 & 0 & 8.2134 & 0 & 8.2134 & 32.8818 & 8.2134 \\
0 & 0 & 0 & 0 & 0 & -8.8209 & 0 & 0 & -8.2134 & 0 & 8.2134 & 25.2923
\end{pmatrix} (min^{-1})$$

$Q = 1500\ m^3/hr$

$$[B] = \begin{pmatrix} 43.1297 & -13.689 & 0 & 13.689 & 0 & 0 & 13.689 & 0 & 0 & 0 & 0 & 0 \\ -15.714 & 56.8024 & 13.689 & 0 & 13.689 & 0 & 0 & 13.689 & 0 & 0 & 0 & 0 \\ 0 & -15.714 & 43.1297 & 0 & 0 & -13.689 & 0 & 0 & 13.689 & 0 & 0 & 0 \\ -13.689 & 0 & 0 & 43.1297 & -13.689 & 0 & 0 & 0 & 0 & 13.689 & 0 & 0 \\ 0 & -13.689 & 0 & -15.714 & 56.8024 & -13.6890 & 0 & 0 & 0 & 0 & -13.689 & 0 \\ 0 & 0 & -13.689 & 0 & 15.714 & 43.1297 & 0 & 0 & 0 & 0 & 0 & 13.689 \\ -13.689 & 0 & 0 & 0 & 0 & 0 & 41.1116 & 13.689 & 0 & 13.689 & 0 & 0 \\ 0 & -13.689 & 0 & 0 & 0 & 0 & 13.689 & 54.7842 & -13.689 & 0 & 13.689 & 0 \\ 0 & 0 & -14.702 & 0 & 0 & 0 & 0 & 13.689 & 42.1241 & 0 & 0 & 13.689 \\ 0 & 0 & 0 & -13.689 & 0 & 0 & -13.689 & 0 & 0 & 41.1116 & 13.689 & 0 \\ 0 & 0 & 0 & 0 & -13.689 & 0 & 0 & 13.689 & 0 & 13.689 & 54.7842 & 13.689 \\ 0 & 0 & 0 & 0 & 0 & -14.702 & 0 & 0 & 13.689 & 0 & 13.689 & 42.1241 \end{pmatrix} (min^{-1})$$